

Final Draft
of the original manuscript:

Nwaogu, U.C.; Blawert, C.; Scharnagl, N.; Dietzel, W.; Kainer, K.U.:
**Influence of inorganic acid pickling on the corrosion resistance of
magnesium alloy AZ31 sheet**
In: Corrosion Science (2009) Elsevier

DOI: 10.1016/j.corsci.2009.06.045

Influence of inorganic acid pickling on the corrosion resistance of magnesium alloy AZ31 sheet

U. C. Nwaogu^a, C. Blawert^{b*}, N. Scharnagl^b, W. Dietzel^b, K. U. Kainer^b

^aTechnical University of Denmark

Department of Mechanical Engineering

Building 425, Room 023,

DK – 2800 Kgs. Lyngby

Denmark

^bInstitute of Materials Research

GKSS-Forschungszentrum Geesthacht GmbH

D-21502 Geesthacht, Germany

* Corresponding author: carsten.blawert@gkss.de

Abstract

Surface contaminants as a result of thermo-mechanical processing of magnesium alloys, e.g. sheet rolling, can have a negative effect on the corrosion resistance of magnesium alloys. Especially contaminants such as Fe, Ni and Cu, left on the surface of magnesium alloys result in the formation of micro-galvanic couples and can therefore increase corrosion attack on these alloys. Due to this influence they should be removed to obtain good corrosion resistance.

In this study, the effect of inorganic acid pickling on the corrosion behaviour of a commercial AZ31 magnesium alloy sheet was investigated. Sulphuric, nitric and phosphoric acids of different concentrations were used to clean the alloy for various

pickling times. The surface morphology, composition and phases were elucidated using scanning electron microscopy, X-ray fluorescence analysis, spark discharge-optical emission spectroscopy, energy dispersive X-ray spectroscopy and infrared spectroscopy. The effect of surface cleaning on the corrosion properties was studied using salt spray test and electrochemical impedance spectroscopy. The experimental results show that acid pickling reduces the surface impurities and therefore enhances the corrosion resistance of the alloy. The cleaning efficiency of the three acids used and the corrosion protection mechanisms were found to be remarkably different. Best corrosion results were obtained with nitric acid, followed closely by phosphoric acid. Only the sulphuric acid failed more or less when cleaning the AZ31 sheet. However, to obtain reasonable corrosion resistance at least 5 μm of the surface of AZ31 magnesium alloy sheet have to be removed.

Keywords: AZ31 magnesium alloy sheet, acid pickling, corrosion rate, surface impurities, corrosion resistance.

1. Introduction

The major challenge in the use of Mg alloys is their high susceptibility to galvanic corrosion attack [1], and even micro-galvanic corrosion of the alloys without contact to other metals is possible due to heavy metal impurities such as iron, copper and nickel. Therefore, corrosion can be minimized by the use of high purity alloys that maintain heavy metal impurities below the tolerance limits. The removal of bad design, flux inclusions, surface contaminations, galvanic couples and the avoidance of inadequate or incorrectly applied surface protection schemes can also significantly decrease the corrosion of Mg

alloys in service [1]. However, processing of these alloys can raise the surface impurity content above the tolerance limits. To this end, the surfaces of Mg alloys are supposed to be pre-cleaned prior to further surface modification in order to enhance their corrosion resistance and surface appearance [2]. Mechanical and chemical cleaning methods are used either separately or in combination, depending on the specific application and product involved [3]. The mechanical cleaning is achieved by grinding and rough polishing, dry or wet abrasive blast cleaning; wet brushing and wet barrel or bowl abrading (vibratory finishing). Chemical cleaning methods for Mg alloys include vapour degreasing, solvent cleaning, emulsion cleaning, alkaline cleaning and acid cleaning. Cleaning processes of either type (mechanical and chemical) require adequate control to ensure repetitive reliability [3]. With regard to our study, a chemical cleaning process using various acids was adopted. However, most of the published work used acid cleaning only as a pre-treatment before further coating steps [4 – 10]. Following the results of these previous studies, the reason why acid pre-treatments can enhance the corrosion resistance of Mg alloys was not elucidated in detail. Therefore, the present study was undertaken to determine the influence of three commonly used acids in cleaning solutions on the surface composition, phases and morphology of AZ31 magnesium alloy sheet. Intentionally, the pure acids without any additional components, e.g. detergents or wetting agents, were used to identify the effect of the acid solely. The findings were correlated with the corrosion behaviour in order to determine the required extent of etching (material removal) for enhanced corrosion resistance of the alloy. The acids HNO_3 , H_2SO_4 and H_3PO_4 investigated in this study were selected based on our own previous studies and from literature [3].

2. Experimental

The substrate investigated is a commercial AZ31 magnesium alloy sheet of 2 mm thickness (as-received; AR) with chemical composition given in Table 1. It should be noted that the bulk of the sheet has a composition according to the standard for AZ31, but that the surface is contaminated with iron and nickel from the processing of this alloy sheet. The sheet was press-cut into two sets of specimens of dimensions 50 mm x 50 mm x 2 mm and 50 mm x 20 mm x 2 mm, respectively, using a Durma MS 2004 Plate shear.

A solution of NaOH for degreasing and three concentrations of each of the acids for pickling were prepared in the concentrations given in Table 2. The selected concentrations for each acid differ, because the medium concentrations and cleaning times were chosen according to the information obtained from literature, assuming that these are almost optimized parameters [3]. Higher and lower concentrations as well as longer and shorter cleaning times were selected accordingly to optimize the pickling solutions for the available AZ31 sheet.

The cleaning process was initiated by immersion of the specimens in a 1 M solution of NaOH for 60 s to degrease the plates (alkaline cleaning). After the alkaline cleaning, the plates were rinsed in deionized water for about a minute and dried in a warm (slightly above room temperature) stream of air. After this pre-cleaning step, a set of three plates were immersed in each of the pickling solutions for the times listed in Table. 2. Finally, these were dipped in 1 molar NaOH solution to neutralize the acid on the specimens and to stop further reaction, followed by rinsing in deionized water and acetone for about one minute respectively. At the end of the process, they were dried in a warm stream of air (as stated above). The specimens (50 mm x 50 mm x 2 mm) were weighed before and after the

cleaning process using a Mettler AC 100 electronic balance. The weight difference was used to estimate the material removed in micrometer (μm) as calculated from the equation (1) below.

$$W = \frac{w \cdot 10^4}{\rho \cdot A} \quad (1)$$

where W = material removed in μm
 w = weightloss in g
 ρ = density in g/cm^3
 A = area in cm^2

Due to the large number of specimens, a screening phase was performed to identify the best and the worst condition for each acid according to the salt spray performance. All specimens were exposed to neutral 5 % NaCl solution fog in a Weiss SC 450 salt spray test (SST) chamber for a period of 48 hours. The corrosion rates (mm/year) were evaluated from weight loss measurements using equation 2.

$$R = \frac{8.7757 \cdot 10^4 \cdot w}{\rho \cdot A \cdot t} \quad (2)$$

where R = corrosion rate in mm/year
 t = time in hours

with the factor 8.7757×10^4 used for unit conversion.

Prior to the corrosion test, the surface roughness and the remaining contamination on the surface of all specimens were determined and the surface appearance was checked by light microscopy. A Hommel Tester T1000, with Turbo Datawin-NT1 software, was used to measure the surface roughness (R_a -parameter). The elemental composition on the surface was determined by spark discharge optical emission spectroscopy (SD-OES) with spark analyzer vision software (SPECTROLAB, version 1.40.002). The composition given is the average of three different runs for each specimen and was obtained from a depth of down to

100 μm from the top surface. This implies that the measured elemental composition is only an average over this depth and the real surface contamination is even higher (about 20 x assuming 5 μm depth of severely contaminated surface). Due to the heavy deformation during rolling the contamination is not only restricted to the top surface, thus especially enrichment of heavy metal impurities can be seen, even if they are "diluted" by the larger analyzed volume.

To further understand the mechanisms of cleaning and improved corrosion resistance, only the best and the worst conditions in salt spray tests were selected for more detailed studies. The surface morphology and composition were examined in a ZEISS Ultra 55 scanning electron microscope (SEM) coupled with Energy Dispersive X-ray Spectroscopy (EDX) detector operating at an accelerating voltage of 15 kV. Further information about the phases, compounds and impurity level on the surface was obtained with an infrared (IR) spectrometer Bruker Tensor 27 with Opus 6.5 software and X-ray fluorescence (XRF) analyzer, Bruker AXS S4 Explorer (Germany) with Bruker AXS SPECTRA plus software (version 1.70). Further corrosion studies were performed using electrochemical impedance spectroscopy (EIS). A typical three electrode cell with 300 ml of neutral aqueous 5 % NaCl solution, a platinum mesh as a counter electrode, Ag/AgCl as a reference electrode and the specimens of AZ31 alloy as the working electrode was used. The EIS measurements were performed at open circuit potential over a frequency range from 10 kHz to 0.01 Hz with a potential amplitude signal of 10 mV after 2 and 20 hours of immersion in the electrolyte, respectively, using a Gill AC potentiostat. Additional EIS measurements were performed in aqueous solutions of 0.01 M Na_2SO_4 or 0.01 M NaNO_3 with and without addition of 0.1 M NaCl after an immersion time of two hours.

3. Results

3.1 Material removal

As expected, the amount of material removed during immersion increased with immersion time (with the exception of specimens cleaned in 50 g/l sulphuric acid) and also with the concentration of each acid as can be seen in Fig. 1. Sulphuric acid treated specimens with 50 g/l did not follow the same trend, and the amount of material removed ($6.85 \pm 1.43 \mu\text{m}$) at this concentration is comparable for all the immersion times. The maximum material removal for sulphuric acid cleaning is $8.01 \pm 1.43 \mu\text{m}$ while the minimum is $0.45 \pm 0.04 \mu\text{m}$. From Fig. 1, it can be seen that for nitric and phosphoric acids the maximum material removal of $8.21 \pm 0.11 \mu\text{m}$ and $4.92 \pm 0.20 \mu\text{m}$, respectively, was observed at the highest concentrations and longest immersion times while the minimum material removal of $0.35 \pm 0.06 \mu\text{m}$ and $0.76 \pm 0.11 \mu\text{m}$, respectively, was observed at the lowest concentrations and shortest immersion times. Looking at the cleaning rates obtained for the three acids (Fig. 2) it is obvious that the rates are reduced with increasing cleaning times. The strongest decrease was observed for sulphuric acid, followed by phosphoric acid, and the lowest decrease was found for nitric acid.

3.2 Surface appearance and roughness

With the cleaning and removal of material from the surface of the AZ31 sheet the optical appearance changed depending on the acid used for cleaning. In phosphoric acid a dark greyish surface appearance was observed, while in nitric and sulphuric acids the alloy surface had a more metallic look. However, nitric acid cleaning gave the shiniest metallic appearance. The surface appearance was generally closely related to the surface roughness

and Fig. 3 shows the R_a values of the cleaned specimens as a function of the acid used for cleaning and of the amount of material removed from the surface. For comparison, the values of as received specimens are also displayed. Interestingly, for all acids the surface roughness was reduced from 0.44 ± 0.15 to about $0.25 \mu\text{m}$ if not too much material is removed. However, for sulphuric acid the R_a values increased quite rapidly with increasing material removal, reaching more than $2 \mu\text{m}$ after about $7 \mu\text{m}$ material removal. The best results were obtained with nitric acid reducing the surface roughness to about $0.25 \mu\text{m}$, independent of the amount of material removed (up to $8 \mu\text{m}$) and suggesting that the etching was quite uniform. For phosphoric acid similar low R_a values were found, but only if not more than $2.0 \mu\text{m}$ material was removed from the surface. With increasing material removal ($> 2.0 \mu\text{m}$) the R_a value started to increase continuously reaching $0.75 \mu\text{m}$ for $5 \mu\text{m}$ material removal.

3.3 Surface impurity level

The composition determined in the bulk and on the surface of the commercial AZ31 Mg alloy sheet by SD-OES (Table 1) clearly shows that the surface of the commercial AZ31 specimens is contaminated mainly with Fe and Ni. Contamination with copper is not a problem. However, it can be expected that the increasing material removal from the surface of the specimens would reduce the surface impurity level, although this expected trend was not that clear.

The change of surface impurity levels of each of Fe, Cu and Ni with the material removed for each acid and for all the conditions investigated is presented in Fig. 4. From Fig. 4a, it can be seen that the copper impurity level of the surface is close to the bulk composition,

which is much lower than the impurity level of the standard (Table 1). However, a slight but by far not critical increase in the copper content is visible for all acids. Comparing all three acids, phosphoric acid treatment seems to have a slightly higher enrichment with increasing removal of material. Fig. 4b presents the iron impurity level depending on the amount of material removed. It can be seen that there is reduction in impurity level for all the treated specimens relative to the as-received specimens, but only treatments with sulphuric acid reach iron impurity levels comparable with the standard, while nitric and phosphoric acid treatments are only approaching the standard without reaching it. However, the etching behaviour of the highest concentration of sulphuric acid is somehow unpredictable, showing with increasing material removal (not correlating with longer cleaning times) an increase in the iron level again. It is also observable that the two acids (nitric and sulphuric acid) which form soluble iron salts (Table 3) showed more reduction in the iron impurity level than phosphoric acid (Fig. 4b). Looking finally at the nickel impurities it is quite evident from Fig. 4c that increasing material removal reduces continuously the nickel impurity level and standard as well as the lower bulk concentration levels can be reached for all acids.

3.4 Salt spray corrosion (SST)

The variation of the salt spray corrosion rates with the amount of material removed in the three acids is shown in Fig. 5. The corrosion rates of an as-received specimen (not cleaned) are displayed for comparison. It can be seen that all the corrosion rates of the cleaned specimens (except in 10g/l sulphuric acid) were significantly reduced as material removal increased and the impurity level decreased. However, it is also obvious that sulphuric acid

was less effective in reducing the corrosion rate of AZ31 compared to phosphoric or nitric acid. Considering the same amount of material removed, AZ31 revealed up to 10 times higher corrosion rates after sulphuric acid cleaning compared to cleaning with the other two acids. However, as shown in Section 3.3 all three cleaning processes were effective in the removal of the surface contaminants and heavy metal impurities that are deleterious to the corrosion behaviour of AZ31 magnesium alloys, although the reason for this finding is not obvious. With the used cleaning parameters no satisfying corrosion resistance (defined by a corrosion rate of about 1 mm/year) was obtained with sulphuric acid, even if 8 μm of material was removed from the surface. In contrast, for the other two acids the removal of 4 – 5 μm of material from the surface was sufficient to obtain corrosion rates less than 1 mm/year. This suggests that further mechanisms, apart from impurity removal, have an influence on the corrosion resistance.

To understand the cleaning mechanisms as well as the influence of the different acids on the surface modification and thus on the corrosion resistance, more detailed microstructural studies were performed on specimens for each acid showing the lowest and highest corrosion rates in SST. The selected specimens and their cleaning conditions are displayed in Tables 4 and 5. For nitric acid the lowest corrosion rate of 0.51 ± 0.10 mm/year was obtained when 8.21 ± 0.11 μm of material was removed. Phosphoric acid followed with a corrosion rate of 0.74 ± 0.31 mm/year and 4.14 \pm 0.35 material removed and finally sulphuric acid with a corrosion rate of 2.20 ± 0.18 mm/year at 6.85 ± 0.85 μm removed (Table 4). The worst corrosion behaviours (Table 5) was found for sulphuric acid treated specimen with a corrosion rate of 17.16 ± 0.74 mm/year, followed by nitric acid treated specimens with a corrosion rate of 10.10 ± 4.44 mm/year and finally phosphoric acid with a

corrosion rate of 7.76 ± 1.00 mm/year. In all those cases less than 2 μm material was removed from the surface, suggesting that not all of the impurities were removed from the surface so that the cleaning was not sufficient.

3.5. Surface morphology

A comparison of the surface of an as-received specimen and cleaned specimens is presented in Fig. 6 and 7, respectively. A closer look on the surface of the as-received specimen (Fig. 6) shows the presence of randomly distributed deposits/particles and scratches indicating the rolling direction. A comparison with the surface of the treated specimens (Fig. 7) shows that there is clear evidence of cleaning on specimens showing good corrosion resistance as all the scratches are removed. However, each acid creates a typical surface appearance. The surface cleaned in sulphuric acid (Fig. 7a) does not reveal the typical grain structure of the AZ31 and it seems as if there is either quite uniform removal of material or, more likely, a thin deposited layer with micro-cracks uniformly distributed across the surface. These micro-cracks are supporting the idea of a thin deposited film which can crack when the surface dries after the cleaning process. However, it should be kept in mind that the best corrosion resistance was only obtained for short cleaning times. Overall, the surface still looks rough and dirty, with quite a large number of particles left on the surface.

Longer treatment times comparable to those of other acids result in surfaces similar to the one shown in Fig. 8. The magnesium matrix material is uniformly removed, but there are intermetallic precipitates remaining on the original surface level. These were not undermined by the etching treatment and are sticking out of the surface explaining the

increasing surface roughness and decreasing corrosion resistance observed. In contrast, the specimens cleaned in nitric acid were strongly but relatively uniformly etched and the typical microstructure of AZ31 with grains and grain boundaries became visible (Fig. 7c). The surface looks reasonably clean with only a few particles and deposits left on the surface. This is consistent with the observed shiny metallic optical appearance. After phosphoric acid cleaning the surface (Fig. 7e) is covered with small island patches, which are most likely phosphates deposited on the surface. This morphology is similar to the surface appearance of phosphate conversion coatings on magnesium alloy AZ91D as reported by Zhou et al. [11]. The formation of this surface layer may have impeded further dissolution of the substrate by creating a barrier between the substrate and the cleaning solution, explaining the lowest amount of material removal for phosphoric acid.

All of the sufficiently cleaned surfaces (except those cleaned with sulphuric acid) reveal a clear reduction in the amount of particles or deposits on the surface. There are holes in the surface which were previously occupied by the particles. Due to the etching and the galvanic effect the matrix was removed and these were fallen out of the surface. The presence of particles for which the process of being removed from the matrix was interrupted is also visible. The etching/cleaning time was not long enough to remove the whole matrix around these particles, so that they are still sticking in the surface, surrounded by a trench of enhanced removed matrix. However, for sulphuric acid this undermining of particles was not observed. The material around the particles was removed, but the removal proceeded not underneath the particle so that they were not falling out of the surface, but remained on the surface.

Turning to the surface appearance of specimen with the poorest corrosion resistance it is clear that there was not sufficient cleaning progress because the cleaning times were too short and/or the concentration of the acid was too weak. The surface cleaned in very diluted sulphuric acid (Fig. 7b) has still the same deposits/particles on the surface as the as-received material, even though the scratches were removed. Similar features are visible for nitric acid (Fig. 7d), when low concentration of the acid and the cleaning time was not enough to allow for sufficient material removal. Even the scratches were not completely removed, and the structure-less, strongly deformed top surface is still visible as only 0.35 μm where removed. For phosphoric acid the surface appears to be free from any surface coverage, and removal of about 0.75 μm was obviously sufficient to remove the scratches and the strongly deformed top layer (Fig. 7f). However, some contaminants and particles are still present on the surface. Some micro-cracks are also visible indicating that probably a thin phosphate film already exists on the surface which cracks when the film dries.

3.6 Surface phases and elemental composition

The infrared spectra taken from the surfaces of an as-received specimen and cleaned specimens are presented in Fig. 9. The spectra of cleaned specimens (Fig. 9b-d) have some bands similar to those present in the spectrum of the as-received specimen (Fig. 9a). In addition, the spectra of cleaned specimens show bands emanating from the products (salts) of the reaction of the acids with the substrate elements. The bands similarity in the spectra is characteristic of a series of closely related (iso-structural) compounds [12]. The compounds present on the surface of cleaned specimens according to the acid used include sulphates, nitrates or phosphates of the major divalent and trivalent metals. Their oxides

and hydroxides are also present, but at a lower intensity. There is also presence of carbon dioxide (CO₂) gas due to adsorption of the atmospheric carbon dioxide on the surface of the substrate or CO₂ belonging to the unsatisfying background compensation since the analytical chamber was not evacuated with nitrogen. Some of this CO₂ will react with moisture to form carbonates on the surface of the specimens.

The possible reaction products between the alloy and the cleaning solutions are given in Table 3. The solubility constants K_{sp} of the possible compounds (salts) are provided to estimate whether a protective film may form on the surface of the substrate. From the information given in Table 3 for the alloying elements and the base metal, all the sulphates and nitrates formed are soluble in aqueous solution; therefore, it is unlikely that they will form protective films on the surface of the substrate. However, the phosphates of the alloying elements and of the base metal are insoluble. This means that phosphate films composed of alloying elements and of the base metal are possibly formed on the surface of the substrate (Fig.7e). This might create a protective layer on the surface of the substrate. Formation and stability of Mg phosphate ($K_{sp} = 1.04 \times 10^{-24}$) should be better than those of the phosphates of the alloying elements (for Al phosphate, $K_{sp} = 9.84 \times 10^{-21}$ and Zn phosphate is slightly soluble). There is also hydroxide film formation on the surfaces of the substrate after the cleaning process, mainly due to the neutralisation after the acid cleaning done in 0.1 M NaOH solution, but also due to the reaction of the cleaned surfaces with water vapour or moisture. These hydroxides are more or less insoluble in aqueous solution at the neutral pH of the corrosive medium and can provide additional protective coverage on the surface of the substrate. However, from the hydroxide peaks in the spectra (Fig. 9), the amount appears to be quite low. Furthermore, it is evident that remains of the cleaning

operation exist on the surface even for the soluble compounds, thus SO_4^{2-} and NO_3^- anions were detected on the surface, but at much lower levels compared to PO_4^{3-} . The real amount can not be determined with the characterisation methods available, but at least traces of them were still present.

Additional information about the elements present at the surfaces was gained by XRF analysis, shown in Fig. 10. All surfaces reveal a significant percentage of oxygen (Fig. 10a). The source of this oxygen could be the acid anions, CO_2 and probably the presence of oxides and hydroxides which formed during neutralisation and during storage after the cleaning process. Support for the assumption of phosphate layer formation is visible in the surface enrichment with phosphorus (Fig. 10b) and also the enrichment of the surface with sulphur in the case of sulphuric acid cleaning (Fig. 10c), suggesting the presence of sulphate anions is confirmed. This is consistent with the results from IR spectroscopy (Fig. 9). Due to the limitation of the instrument, nitrogen could not be detected on the surface of the specimen treated with nitric acid.

Finally, some EDX point or spot analyses of the surfaces of the as-received and treated specimens were performed to determine where and in which form the impurities were present on the surface. The elemental compositions for typical particles/phases detected on the surfaces before and after the various cleaning treatments are presented in Table 6. The iron contamination of the as received material is so high and uniformly distributed over the surface that in most of the cases iron could be detected in the matrix of the alloy. Due to the reduced material removal and enhanced phosphate film formation the removal of iron impurities was reduced in the case of phosphorous acid cleaning, thus it can still be detected in the matrix. Only for nitric and sulphuric acid most of the matrix analyses reveal

no presence of iron. Furthermore, from the elemental composition of the matrixes, it can be concluded that there is no formation of a thicker film (except a thin oxide layer) on the surfaces except for specimens treated with phosphoric acid . The elemental compositions correlate with the expected standard of AZ31, and only the surface after phosphorous acid cleaning showed higher levels of aluminium, phosphorus and oxygen. The phosphorus content detected by EDX analysis is in agreement with the results of the XRF which shows surface enrichment in phosphorus (Fig. 10b). However, there were a couple of other phases visible on the surfaces of the specimens. Impurities such as pure iron, iron oxides, copper and iron enriched particles and carbon rich debris were visible on the surfaces of the as-received sheet. Even though their number was reduced after the cleaning process compared to the as-received material (Fig. 9a) these were still present after the cleaning (Fig. 9b-d). Some of them were deeply pressed into the matrix due to the rolling of the sheet, and obviously the material removal was not deep enough to completely remove them; thus, some were still sticking in the surface. Only the carbon rich debris adhering to the top of the surface was quite easily removed and could not be detected anymore on the specimens which had been sufficiently cleaned.

3.7 Tolerable surface impurity levels

As the impurities were not completely removed, the following analysis should help to identify tolerable impurity levels at the surface in order to guarantee sufficiently low corrosion rates (preferentially less than 1 mm/year). The impurity levels of Fe, Cu and Ni determined by spark discharge-optical emission spectroscopy from specimens showing best and worst salt spray corrosion resistance are shown in Fig. 11. The impurity level after

cleaning is compared with the content measured on the surface (AR) and in the bulk (after removal of 500 μm by grinding) of as-received specimens representing the maximum and minimum contamination of the AZ31 alloy, respectively. It becomes obvious that all cleaning treatments lowered the iron and nickel contents, but the low levels of bulk material were not reached especially for iron. This is consistent with the EDX point analyses showing that impurities on the surface could still be found even after performing the best cleaning treatments used in this study. However, certain limits which can be much higher than the bulk content have to be reached in order to guarantee reasonable corrosion resistance. From Fig. 11a these levels can be defined as < 100 ppm Fe and < 15 ppm Ni. It should be noted that these values are average values, collected from a depth of down to 100 μm from the top surface, and thus the values measured close to the surface might be even higher. Such low impurity levels in combination with low corrosion rates can only be obtained with nitric and phosphoric acid treated specimens. This could be attributed to the extent of etching for nitric acid and to mainly protective phosphate film formation for phosphoric acid. For sulphuric acid treatment, no corrosion rates lower than 2 mm/year were observed even if the above specified tolerance levels were achieved. In contrast, the corrosion resistance decreased with increasing cleaning times and with reduced impurity levels. Hence, the results of sulphuric acid in Fig. 11a were taken after 15 s of etching and not for 120 s as for the other two acids. From this unexpected result it must be concluded that sulphuric acid is not suitable for cleaning AZ31 sheet if bare corrosion resistance is required. Most likely this is related to the observed peculiar etching behaviour not removing noble intermetallic phases from the surface and thus creating sources w strong galvanic corrosion on the surface.

The copper level even on the surface of the as-received condition was very low and was not a problem at all. Therefore, cleaning with all the acids had no real effect on the copper impurity level. Some results indicate slightly higher levels after cleaning, which might indicate some enrichment of copper at the surface after etching (re-deposition of Cu metal on the surface during etching) or, even more likely, just variations of the alloy composition. Carbon is another element that was found on the surface of the as-received sheet. However, compared to the other impurities it is not penetrating deep into the surface and remains obviously on the surface. Thus it can easily be removed by all the cleaning treatments and there is no need to define tolerance limits for carbon.

3.8 Electrochemical properties

The electrochemical properties were elucidated using electrochemical impedance spectroscopy (EIS). The plots in Fig. 12 a and b show the EIS (Nyquist) spectra obtained after 2 and 20 hours of exposure to neutral 5 % NaCl solution from specimens cleaned with the best condition from SST for each acid. From both figures it can be seen that the specimens exhibited one capacitive loop in the high frequency region, indicating similar corrosion mechanisms [13]. This loop is attributed to charge transfer process (Mg^{2+} going into the solution) occurring at the substrate/electrolyte interface [13-15] or to the corrosion behaviour of the surface film [14, 15]. For simplicity, the real impedance and the solution polarization resistance (R_s) (taken where the phase shifts are zero and thus the imaginary parts vanish) were used to calculate the charge transfer resistance (R_p) which is regarded as a measure of corrosion resistance [15]. Generally, in all the plots a negative value of the imaginary impedance was recorded as shown in Figs. 12. This is an inductive behaviour of

the surface which is attributable to the change in the corrosion potential of the substrate/solution interface with time. This inductive behaviour shows that the corrosion initiates as a localized corrosion in the form of pits [16]. The Nyquist plots in Fig. 12a clearly revealed larger R_p values after 2 hours of exposure to 5 % NaCl solution for the treated specimens than for the as-received specimen. From this figure it can be seen that the specimen treated with phosphoric acid show higher R_p values than the specimens treated with other acids. This might be attributable to the combination of impurity removal by etching and phosphate film formation, respectively. It can also be seen that specimens cleaned in sulphuric and nitric acids showed intermediate R_p values which means that they still have some surface impurities but on a much lower level compared to the as-received specimens. The inductive parts of the Nyquist plots indicate that surface impurities were still present on all specimens, causing the localised corrosion attack. Fig. 12b shows an improvement on the R_p values of all the specimens after 20 hours of exposure to 5 % NaCl solution. Phosphoric acid cleaned specimens still have higher R_p values but the specimens cleaned in the other acids showed significant improvement in their R_p values. The reason for this might be that the corrosion process on the surface had removed some of the surface impurities. Localised and galvanic enhanced corrosion around the impurities removed the magnesium matrix around the impurities and these fall to the bottom of the container. Additional hydroxide formation in combination with the above described cleaning effect may be responsible for enhancing the corrosion resistance after longer exposure times to the aqueous solution.

Especially the IR spectroscopy suggested that salts of the respective acids remained on the surface of the specimens. This is obvious for the stable and optically visible phosphate film

that formed during cleaning in aqueous phosphoric acid solutions, but also the other two acids might have had certain amounts of salt remains on the surface even after neutralisation treatment and extensive rinsing in water. To check whether salt remains on the surface could have had an influence on the corrosion resistance, the corrosion behaviour of bulk AZ31 alloy was studied in solutions containing either nitrate or sulphate ions in combination with and without chloride ions. The Nyquist plots obtained in both pairs of solutions are shown in Fig. 13. It is obvious that the corrosion resistance in the sulphate ion containing solution was much lower, which is consistent with the observations made in the salt spray testing. However, even in the presence of chloride ions there no indication of pitting corrosion was found.

4. Discussion

All inorganic acid based cleaning solutions can be adjusted to remove about 5 μm from the surface of the AZ31 alloy sheet within one minute of cleaning operation. This is important as the minimum amount of removal in order to guarantee a sufficiently good corrosion resistance identified by salt spray corrosion performance was 5 μm . However, there are distinct differences between the three acids not only in the cleaning effectiveness but also in the cleaning mechanisms and the final appearance and performance of the cleaned surfaces. This will be discussed in more detail in the following.

Considering the initial cleaning rates it is obvious that sulphuric acid is the most aggressive acid if the concentration exceeds 30 g/l. For the highest concentration an average cleaning rate of 27 $\mu\text{m}/\text{min}$ was determined within the first 15 seconds. The highest phosphoric and nitric acid concentrations used both exhibited similar rates which were remarkably lower

compared to sulphuric acid, namely 7 and 8 $\mu\text{m}/\text{min}$, respectively. However, this is surprising if the effective H^+ ion concentrations (pH values) are considered as an indicator for the cleaning effectiveness. The highest H^+ ion concentration was measured for the nitric acid solution (pH 1.04), followed by sulphuric (pH 1.22) and finally phosphoric acid (pH 1.72) solution. This indicates that the processes at the surface are much more complex and that also the anions may play a crucial role in preventing or not forming protective films. However, the initially very high cleaning rates are greatly reduced for all acids if longer cleaning times are considered. The decrease may be attributed to various aspects which can contribute to different degrees:

- 1) Increasing removal of impurities resulting in more “cleaning resistant” surfaces,
- 2) Formation of protective reaction layers which can reduce the material removal,
- 3) Formation of gas envelopes around the specimens which may reduce or prevent contact with the cleaning solution,
- 4) H^+ ions close to the surface are consumed and have to be replaced over longer distances.

The strongest decrease was observed for sulphuric acid, followed by phosphoric acid and finally the lowest decrease was found for nitric acid. Averaged over a period of two minutes, the best performance was found for nitric acid solution with 4.1 $\mu\text{m}/\text{min}$, followed by sulphuric acid with 3.5 $\mu\text{m}/\text{min}$ and phosphoric acid with 2.5 $\mu\text{m}/\text{min}$. The latter can be clearly correlated with the phosphate film formation on the surface which is partly protective as it grows thicker and denser with increasing exposure to the phosphoric acid based cleaning solution. In nitric and sulphuric acid, such protective reaction layers will not form and hence the other three mechanisms should be responsible for the reduced cleaning

rates. The difference between these two acids is not very large, but the etching by the nitric acid was much more uniform (see roughness) indicating that the strong hydrogen development in the beginning of the cleaning process is detrimental to a uniform cleaning result since it can prevent uniform contact with the cleaning solution and uniform material removal. This leads to heavily etched areas and regions with less etching, resulting in high roughness values as were observed for sulphuric acid if the cleaning time increases. In contrast, nitric acid showed a very uniform etching, indicated by a constant surface roughness independent of the cleaning time, which is also consistent with the nice and shiny metallic surface appearance. Actually, the average roughness values were better than those of the as-received sheet.

Phosphoric and nitric acid showed in the beginning a similar capability to remove material, but at the end phosphoric acid was less effective in material removal if longer cleaning times are considered. This is a result of the film formation on the surface which is also visible in an increasing surface roughness with longer cleaning times. As the layer forms and grows, small single nodal like precipitates form and increase in size and thickness which is reflected by the increasing roughness values. These values are much lower compared to those for sulphuric acid, but higher than those for nitric acid. Another possible disadvantage of the phosphoric acid treatment is the change in colour to dark grey associated with the film formation and the loss of the shiny metal appearance observed for nitric acid and partly also for sulphuric acid.

The removal of material was not the primary objective, this being still the reduction of surface impurities in order to guarantee a good corrosion resistance. Our studies showed that the surface is mainly contaminated with heavy metal contaminations (particles) and

debris (rich in carbon), which have to be reduced or removed in order to obtain the above objective. As the material removal is a question of cost, only the amount absolutely necessary should be removed. A first estimate of how much this needs to be can be obtained from the specified composition standard of the AZ31 alloy or from the composition of the bulk. The fact that mainly iron and nickel are enriched indicates that the contamination is due to the rolling process. In spite of this fact also copper was included in the observation to check whether noble metals may enrich during the cleaning/etching process. The bulk of the alloy contains about 15 ppm of Cu which is by far not critical, and even after the longest etching time of 2 min none of the treatments resulted in contents higher than 25 ppm Cu which is still considered to be harmless for the corrosion resistance. The slight increase might result from surface enrichment, as more noble precipitates containing Cu will not dissolve that easily, and/or from the redeposition of Cu if it was once dissolved, due to the much higher electrochemical potential. Furthermore, there seems to be a slightly higher Cu concentration after cleaning with phosphoric acid which might be due to the insolubility of the copper phosphate (Table 3) resulting in enhanced nucleation or redeposition of nickel containing phosphate compounds on the surface of the substrate.

The iron and nickel contents show more or less the expected reduction of their content with increasing cleaning time/material removal for all acids. However, after cleaning with phosphoric acid the iron content remained much higher. Beside the fact that this acid removed less material, another aspect might be that iron also forms insoluble phosphate compounds which may remain or re-deposit on the surface. The same would be expected for nickel, but due to the much lower overall content re-deposition may not play a crucial role. This leads to the question how the impurities are actually removed. Are they

dissolving as ions or do they precipitate on the surface when the magnesium matrix is dissolving around them during the cleaning process? The observation of the surface before and after the cleaning treatment suggests that the latter is the main process. On the surface of the as-received sheet there are various particles which are pressed into the substrate and debris that seems to sit on the surface. The relative loose debris is removed quite easily. Some of the particles deeper pressed into the substrate were still visible with rings of enhanced removed matrix surrounding them after the cleaning operation. Some smaller particles were fallen out of the matrix, with the remaining holes indicating their former positions. Furthermore, due to the more negative electrochemical potential of the surrounding magnesium matrix, dissolution of the impurities should be negligible as long as they are in contact with the matrix. However, once having dropped down to the bottom of the cleaning containers they may slowly dissolve, increasing the level of heavy metal ions in the cleaning solutions and adding to those which go directly from the surface into solution.

Also of importance for the cleaning operation are the compounds formed by the impurity elements with the respective acids (Table 3). As can be seen, the sulphates and nitrates of the impurity elements are all soluble in aqueous solution. This means that such compounds will most likely not form on the surface and that the heavy metal ions will dissolve into the solution keeping the metal cations (Fe, Cu and Ni) on the surface at lower levels. The phosphates of these impurity elements are insoluble in aqueous solution and may be partly incorporated into the phosphate deposit forming on the surface of the specimens. However, in all cases re-deposition of impurity elements might occur as impurity ions can easily be reduced by the dissolving Mg, especially if the impurity concentration in the cleaning

solution increases during longer cleaning operation. Here, the phosphate solution may have an additional advantage if heavy metal ions once dissolved precipitate from the solution before they can re-deposit on the surface. The concentration effect of dissolved heavy metal ions in the different cleaning solutions will be subject of future studies aiming at answering these remaining questions.

As in the present study fresh solutions were used for each cleaning experiment, it is not really surprising that was no indication for re-deposition of dissolved impurities from the cleaning solution was found. There was no chance that sufficient heavy metal ions were enriched in the cleaning solutions. Thus, as re-deposition of impurities may not play a major role it should be possible to achieve the bulk compositions for longer cleaning times. Therefore, an additional experiment was performed with the optimised nitric acid cleaning conditions but with cleaning times extended to five minutes. The results indicate that the low impurity levels of the bulk can be obtained at least if a fresh etching solution (without major heavy metal concentrations) is used.

Looking at the corrosion rates, it is obvious that with increasing removal of the contaminated surface the corrosion resistance increased for all the acids. This is consistent with a reduction of the impurity level. However, the performance of the specimens cleaned in the various acids was different. The best performance in salt spray testing was observed for phosphoric acid and nitric acid cleaning, with the specimens cleaned in the latter acid performing slightly better. By far the worst performance was observed for sulphuric acid cleaning. The good performance of nitric acid cleaned specimens is not surprising as the impurity levels were rather low and the overall surface appearance looked clean, smooth, metallic, and the etching was quite uniform. It is the performance of the other two acids

which was to some extent unexpected. Even though after sulphuric acid cleaning the surface was rougher and the etching was not that uniform, the obtained impurity levels were even lower than those for nitric acid. Thus, one would expect a corrosion performance being at least comparable to that of the nitric acid. This was not the case, and the reason is not really obvious. A possible explanation might be the observation that the undermining process of noble particles during sulphuric acid pickling was limited compared to that in nitric and phosphoric acid. The particle number at the surface remained much higher, thus enhancing galvanic effects and reducing the corrosion resistance compared to that resulting from the other two pickling treatments. Furthermore, the remains of sulphates and nitrates on the surface which were observed in the IR spectra even after extensive neutralisation and rinsing in water may have had an additional effect. The electrochemical studies (Fig. 13) suggest that in the presence of sulphate less corrosion resistant films formed compared to the presence of nitrate. Combinations with 0.1 M chloride ions yielded no evidence that the film formation was greatly affected and that localised corrosion was promoted within 2 hours of exposure. The phosphoric acid lead to a good corrosion resistance comparable to that achieved by nitric acid, even though the amount of material that was removed was the lowest and the remaining impurity level was the highest of all three acids. This was obviously compensated by the formation of the magnesium phosphate film on the surface (Fig. 7e) which offered additional corrosion protection.

5. Conclusion

According to the results obtained, the acid cleaning processes significantly reduced the surface impurity levels in AZ31 Mg alloy sheet, thereby reducing the formation of micro-

galvanic cells which decreases its galvanic corrosion susceptibility. However, with reasonable cleaning times and material removal the surfaces were not completely clean, and low impurity levels of the bulk material were not obtained. Nevertheless, to obtain good corrosion resistance for AZ31 Mg alloy sheet (1 mm/year for nitric and phosphoric and 2 mm/year for sulphuric acid), 5 μm etching appears sufficient and would require 1 to 2 minutes of etching time, depending on the concentration of the cleaning solution. This will ensure a reduction in impurity level to tolerance limits less than 100 ppm Fe and less than 15 ppm Ni on the surface of the alloy. Other impurities, such as copper or carbon, are not a problem as their concentration is either too low or they can easily be removed.

Two of the three acids investigated are a better choice for cleaning of AZ31 Mg alloy sheet at the concentrations and cleaning times used if bare corrosion resistance is required. These acids are nitric and phosphoric acids. Even though sulphuric acid showed a reasonable cleaning behaviour, the specimens suffered from poor corrosion resistance although the impurity level was sufficiently low. This might be explained by a less effective removal of intermetallic phases as well as by the presence of sulphate remains on the surface, offering less corrosion protection than nitrate remains or thick insoluble phosphate deposits. Among nitric and phosphoric acids, according to the results of this study, a slightly better corrosion performance was obtained with nitric acid.

6. Acknowledgement

The work was carried out at GKSS –Forschungszentrum Geesthacht GmbH, Max-Planck-Strasse 1, 21502 Geesthacht, Germany. Mr. Ugochukwu Chibuzoh Nwaogu is grateful to the European Commission for the scholarship for his studies for Joint European Masters in Materials Science (EMMS).

References

- [1] J. E. Gray, B. Luan, Protective coatings on magnesium and its alloys - a critical review, *Journal of Alloys and compounds*, 336, (2002) 88 - 113.
- [2] N. Shikata, Y. Kondou, Y. Nishikawa, Y. Nishizawa, Y. Sakamoto, T. Fujiwaki, Surface-Treated Article of Magnesium or Magnesium alloys, Method of Surface Preparation and Method of Coating, Patent Cooperation Treaty (PCT), 1999.
- [3] J. E. Hillis, Surface Engineering of Magnesium Alloys, *Surface Engineering ASM Handbook*, 5, (1994).
- [4] C. E. Barchiche, E. Rocca, C. Juers, J. Hazan, J. Steinmetz, Corrosion resistance of plasma-anodized AZ91D magnesium alloy by electrochemical methods, *Electrochimica Acta*, 53 (2007) 417 – 425.
- [5] K. Z. Chong, T. S. Shih, "Conversion-coating treatment for magnesium alloys by a permanganate- phosphate solution, *Material Chemistry and Physics*, 80 (2003) 191 – 200.
- [6] F. Zucchi, V. Grassi, A. Frignani, C. Monticelli, G. Trabanelli, Influence of a silane treatment on the corrosion resistance of a WE43 magnesium alloy, *Surface and Coatings Technology*, 200 (2006) 4136 – 4143.
- [7] R. Supplit, T. Koch, U. Schubert, Evaluation of the anti-corrosive effect of acid pickling and sol-gel coating on magnesium AZ31 alloy, *Corrosion Science*, 49 (2007) 3015 – 3023.
- [8] H. Zhao, Z. Huang, J. Cui, A new method for electroless Ni-P plating on AZ31 magnesium alloy, *Surface and Coatings Technology*, 202 (2007) 133 – 139.
- [9] k. Brunelli, M. Dabala, I. Calliari, M. Magrini, Effect of HCl pre-treatment on corrosion resistance of cerium-based conversion coatings on magnesium and magnesium alloys, *Corrosion Science*, 47 (2005) 989 – 1000.
- [10] H. H. Elsentriecy, K. Azumi, H. Konno, Effect of surface pretreatment by acid pickling on the density of stannate conversion coatings formed on AZ91 D magnesium alloy, *Surface and Coatings Technology*, 202 (2007) 532 – 537.
- [11] W. Zhou, D. Shan, E-H. Han, W. Kei, Structure and formation mechanism of phosphate conversion coating on die-cast AZ91D magnesium alloy, *Corrosion Science*, 50 (2008) 329 – 337.
- [12] S. Aleksovska, V. M. Petrusevski, B. Soptrajanov, Infrared spectra of the monohydrates of manganese (III) phosphate and manganese (III) arsenate: relation to the compounds of the Kieserite family, *Journal of Molecular Structure*, 408/409 (1997) 413 – 416.
- [13] M. Anik, G. Celikten, Analysis of the electrochemical reaction behaviour of alloy AZ91 by EIS technique in H₃PO₄/KOH buffered K₂SO₄ solutions, *Corrosion Science*, 49 (2007) 1878 – 1894.
- [14] H. Ardelean, I. Frateur, P. Marcus, Corrosion protection of magnesium alloys by cerium, zirconium and niobium-based conversion coatings, *Corrosion Science*, 50 (2008) 1907 – 1918.
- [15] K. Y. Chiu, M. H. Wong, F. T. Cheng, H. C. Man, Characterization and corrosion studies of fluoride conversion coating on degradable Mg implants, *Surface and Coatings Technology*, 202 (2007) 590 -598.

- [16] R. Ghosh, D. D. N. Singh, Kinetics, mechanism and characterization of passive film formed on hot dip galvanized coating exposed in simulated concrete pore solution, *Surface and Coatings Technology*, 201 (2007) 7346 – 7359.
- [17] Solubility and solubility product of compounds, *CRC Handbook of Chemistry and Physics*, 78th Edition, David R. Lide, H. P. R. Frederike (Eds.), New York 8 – 106.

FIGURE CAPTIONS

Fig. 1: Variation of material removed by each cleaning bath with immersion time and concentration.

Fig. 2: Variation of cleaning rate with immersion time for sulphuric, nitric and phosphoric acids

Fig. 3: Variation of surface roughness with material removed for various acid.

Fig. 4: Variation of impurity levels with material removed for all the measurements as determined by spark discharge-optical emission spectroscopy.

Fig. 5: Variation of corrosion rates in SST with material removed after cleaning in each acid.

Fig. 6: SEM micrograph of the surface of as-received specimen

Fig. 7: SEM micrographs of selected treatments for each of the acids (a and b for sulphuric acid, c and d for nitric acid and e and f for phosphoric acid, a, c and e, best conditions and b, d and f, worst condtions).

Fig. 8: SEM micrograph of cleaned surface for 120 s in sulphuric acid

Fig. 9: IR spectra of surfaces of as-received specimen (a) and specimens cleaned in various acids (b,c and d).

Fig. 10: Elemental composition on the surfaces of as-received and treated specimens by x-ray fluorescence analysis.

Fig. 11: Composition of impurities detected on the surfaces of as-received (surface), bulk and selected treated specimens by spark discharge-optical emission spectroscopy (a) best and (b) worst corrosion behaviour.

Fig. 12: EIS spectra of as-received and treated specimens with best corrosion behaviour in SST after (a) 2 hours and (b) 20 hours of exposure to neutral 5 % NaCl solution.

Fig. 13: EIS spectra obtained in solutions of 0.01 M NaNO₃ and 0.01 M Na₂SO₄ with or without addition of 0.1 M NaCl

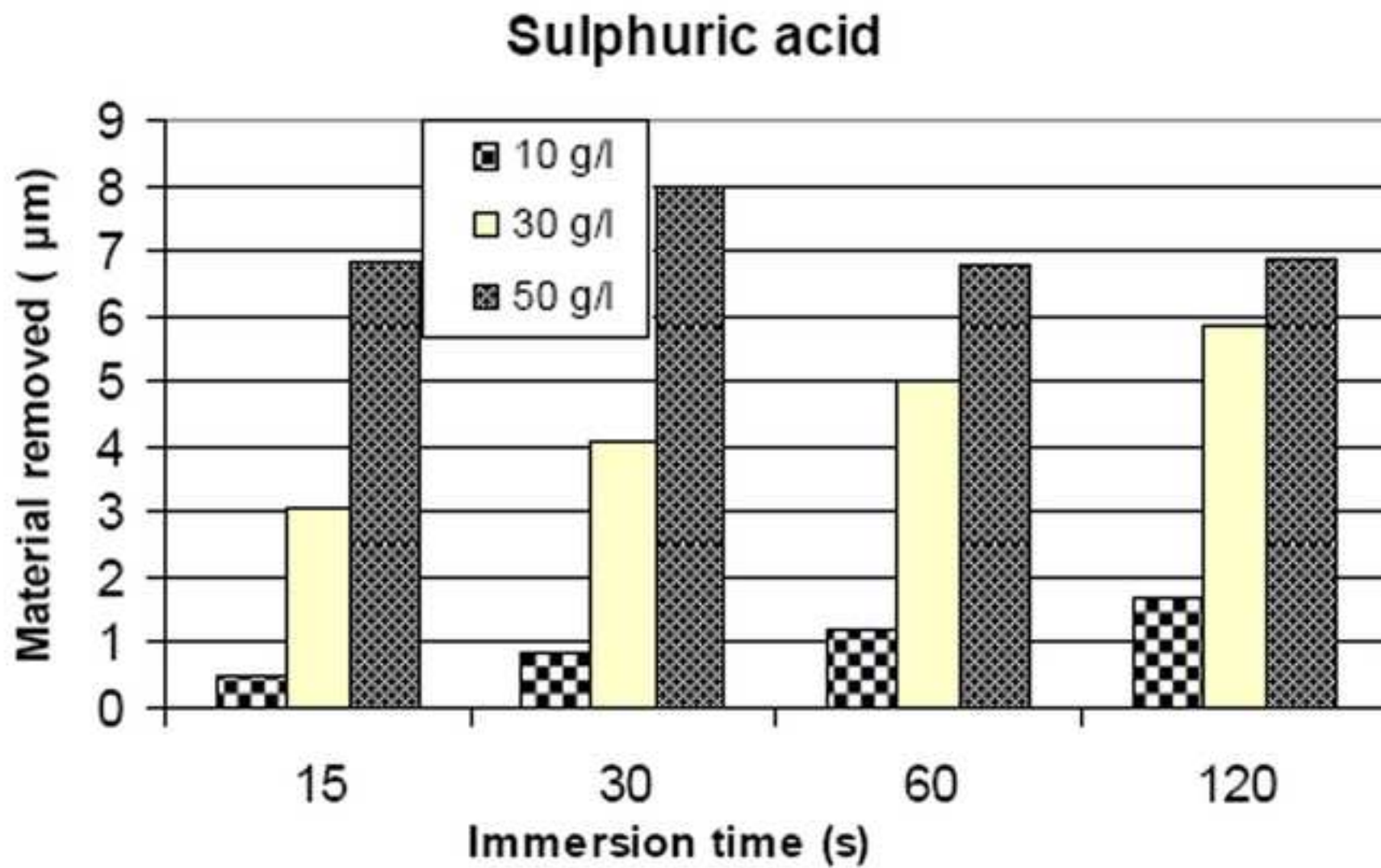


Fig. 1a

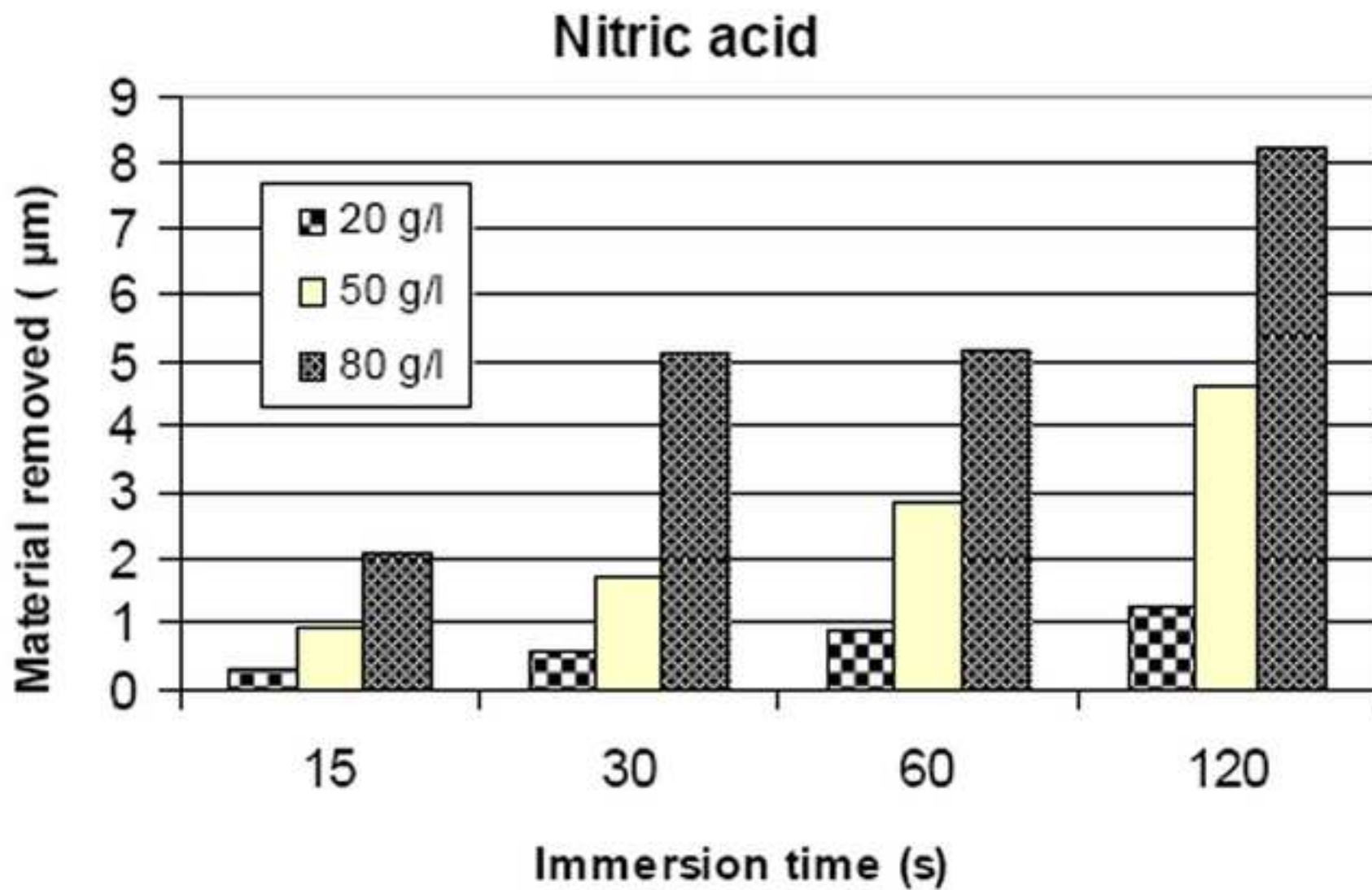


Fig. 1b

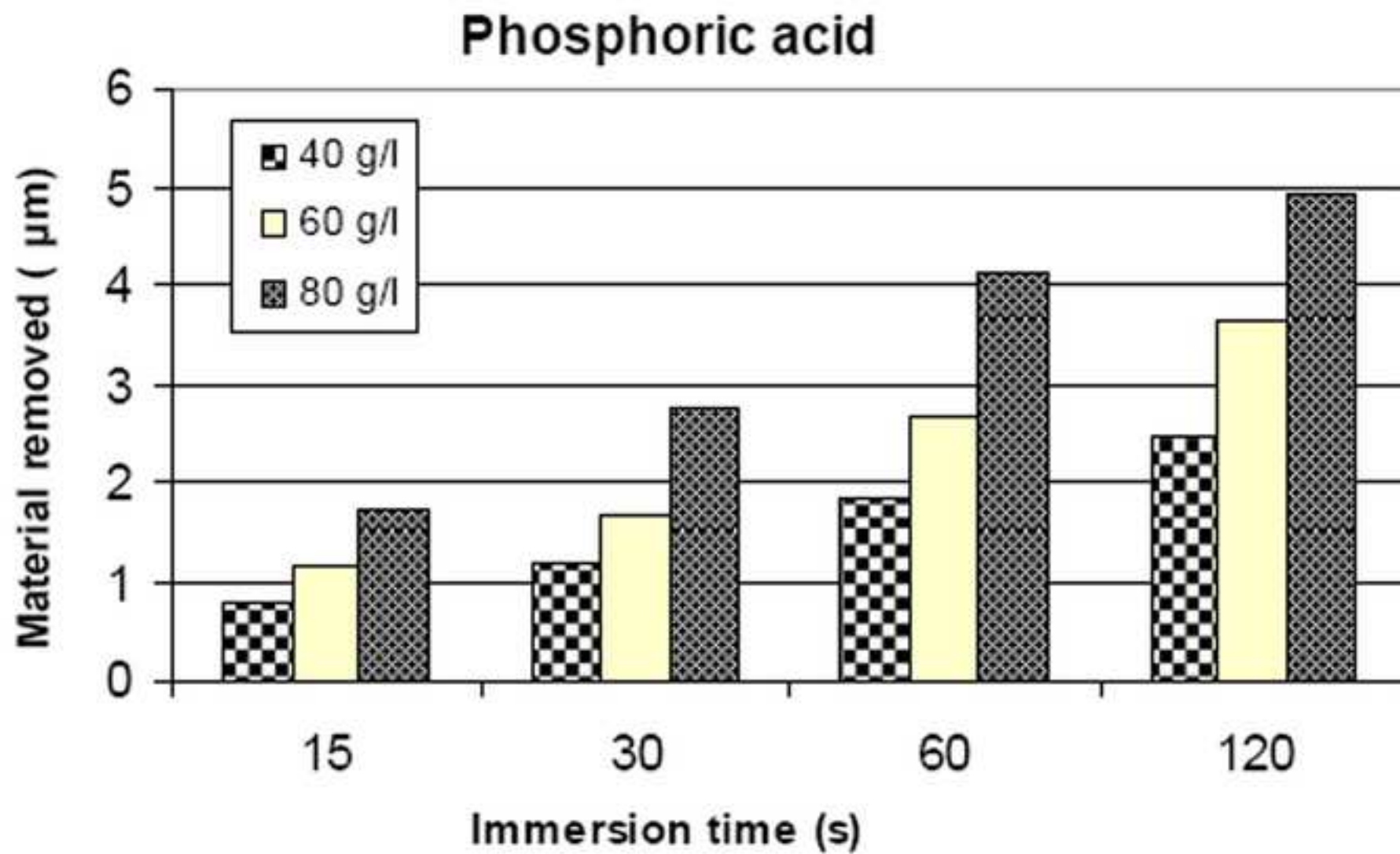


Fig. 1c

Figure 2a

[Click here to download high resolution image](#)

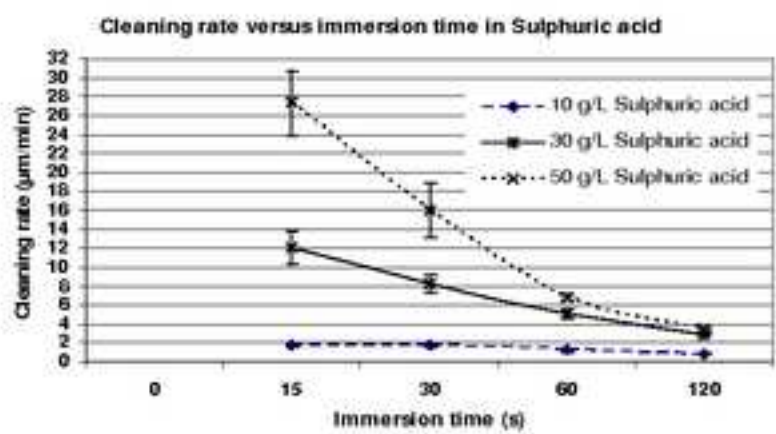


Fig. 2 a

Figure 2b

[Click here to download high resolution image](#)

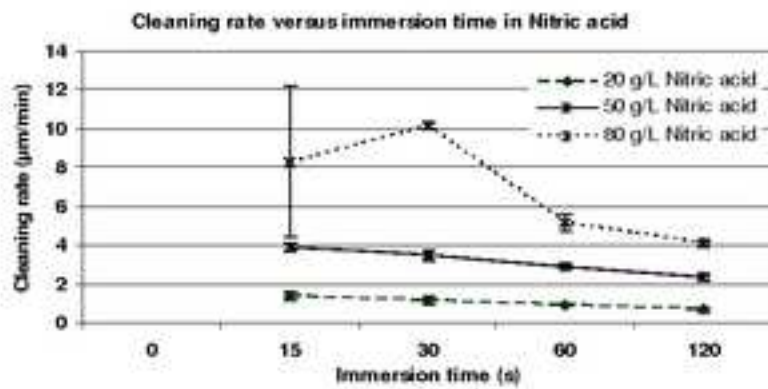


Fig. 2 b

Figure 2c

[Click here to download high resolution image](#)

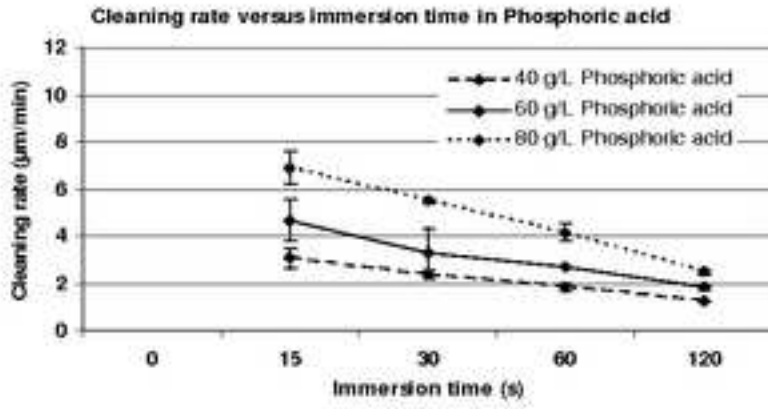


Fig. 2 c

Figure 3

[Click here to download high resolution image](#)

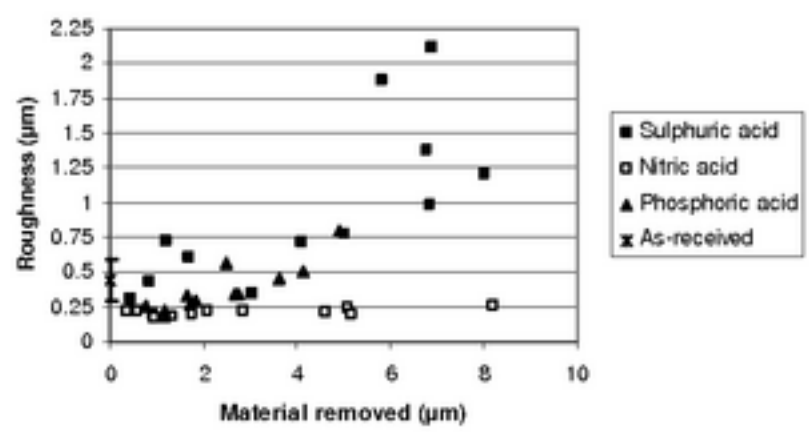


Fig. 3

Figure 4a

[Click here to download high resolution image](#)

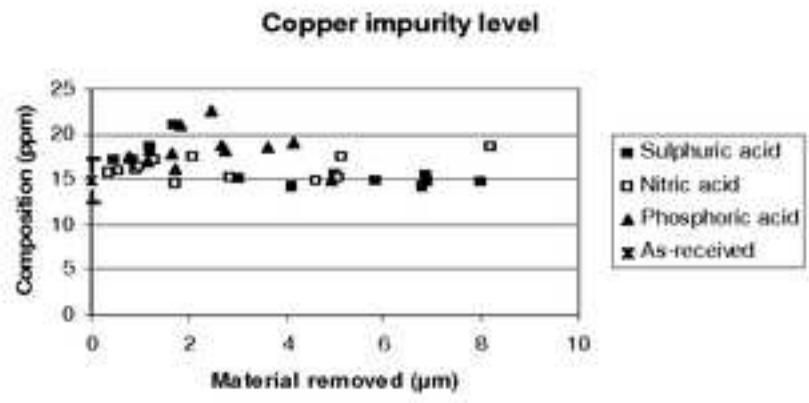


Fig. 4a

Figure 4b

[Click here to download high resolution image](#)

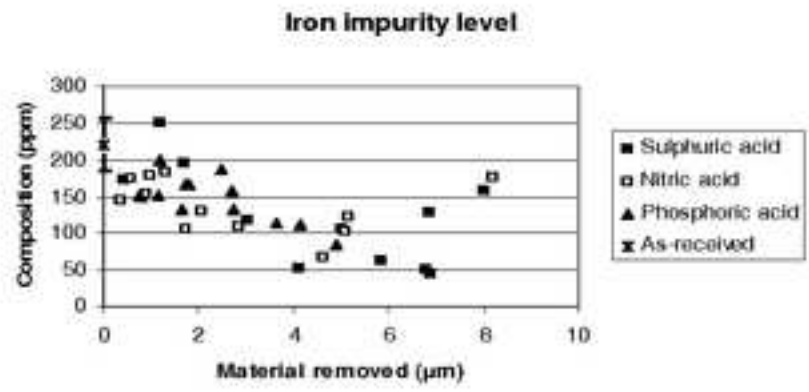


Fig. 4 b

Figure 4c

[Click here to download high resolution image](#)

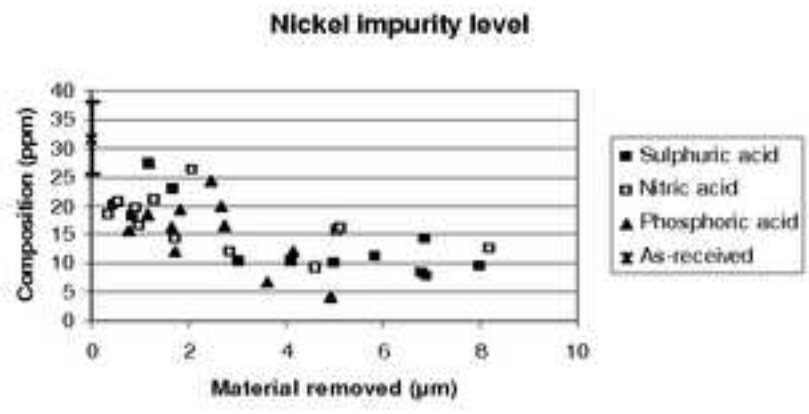


Fig. 4c

Figure 5

[Click here to download high resolution image](#)

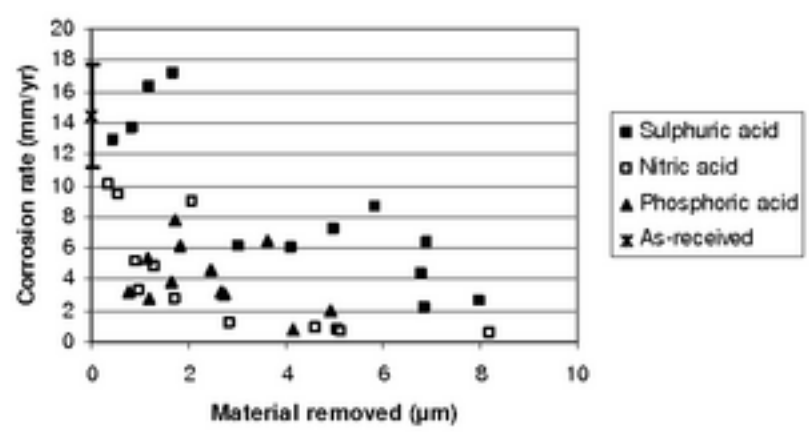


Fig. 5

Figure 6
[Click here to download high resolution image](#)

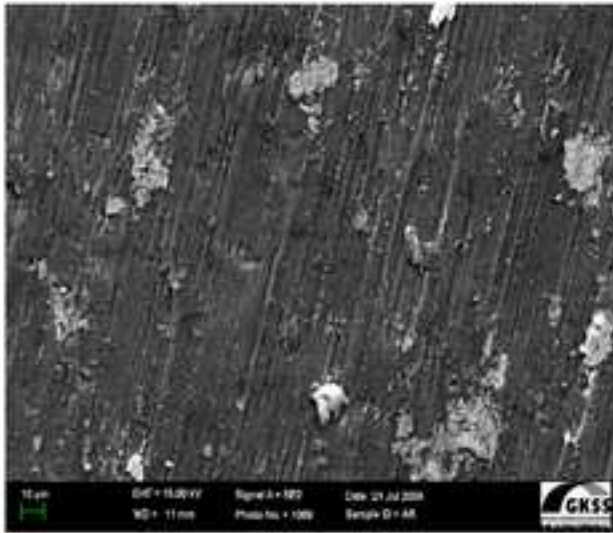


Fig. 6

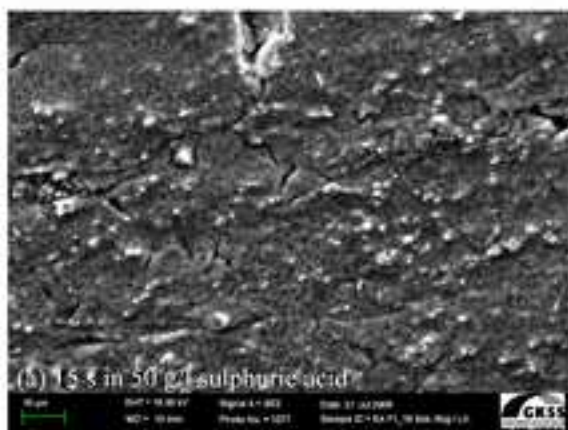


Fig. 7a

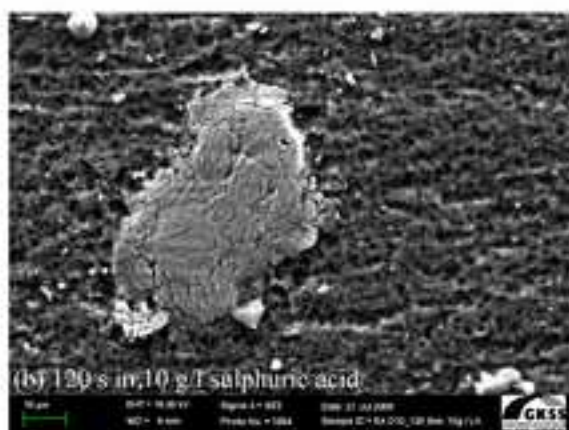


Fig. 7b

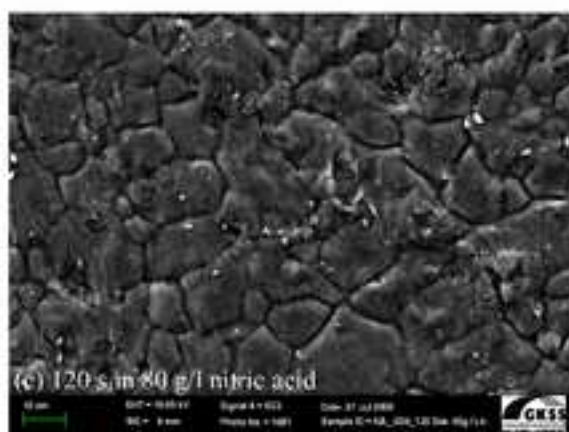


Fig. 7c

Figure 7d

[Click here to download high resolution image](#)

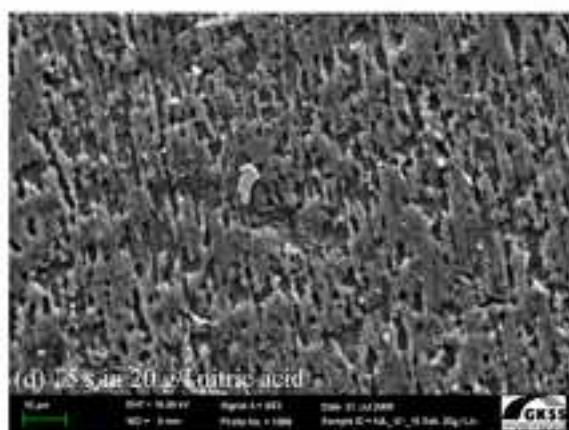


Fig. 7d

Figure 7e

[Click here to download high resolution image](#)

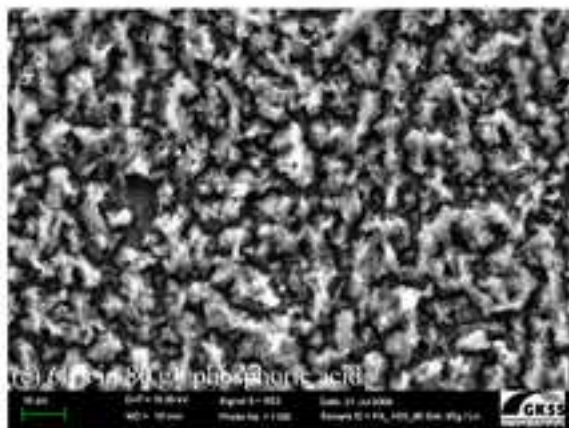


Fig. 7e

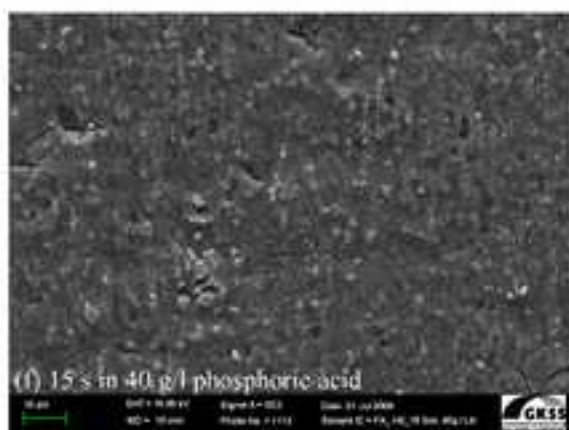


Fig. 7f

Figure 8
[Click here to download high resolution image](#)

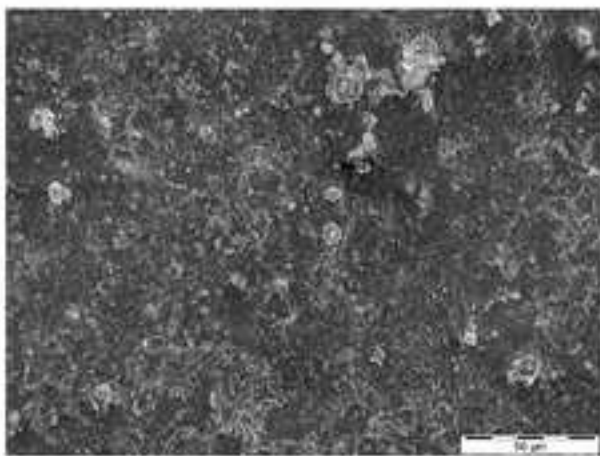


Fig. 8

Figure 9a

[Click here to download high resolution image](#)

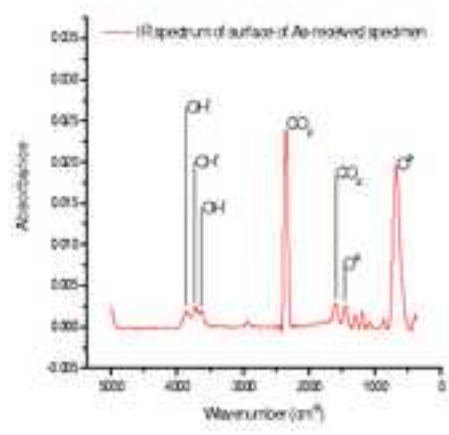


Fig. 9a

Figure 9b

[Click here to download high resolution image](#)

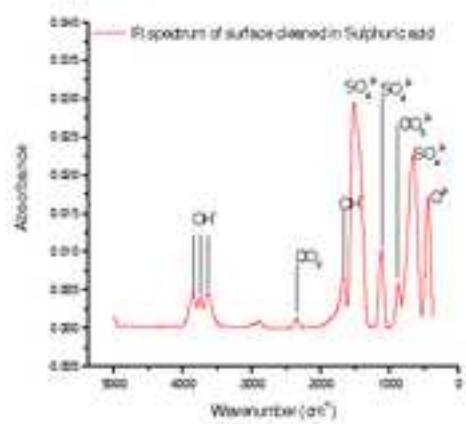


Fig. 9b

Figure 9c

[Click here to download high resolution image](#)

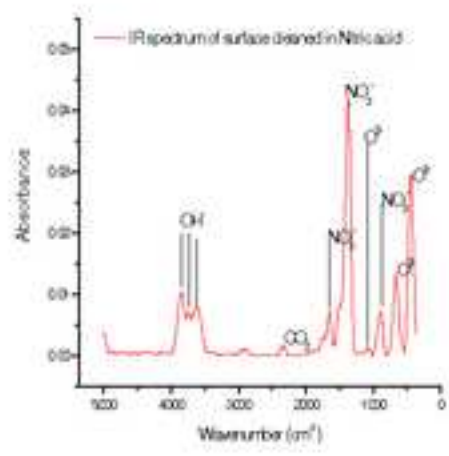


Fig. 9c

Figure 9d

[Click here to download high resolution image](#)

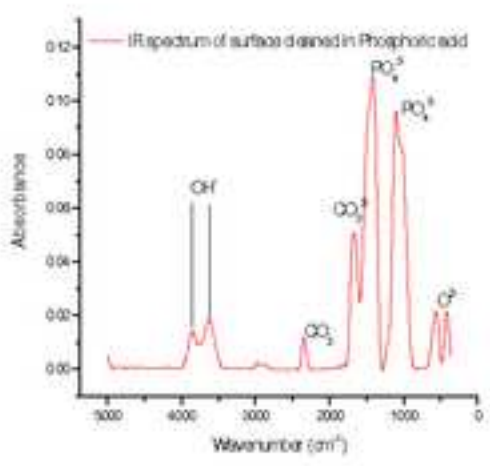


Fig. 9d

Figure 10a

[Click here to download high resolution image](#)

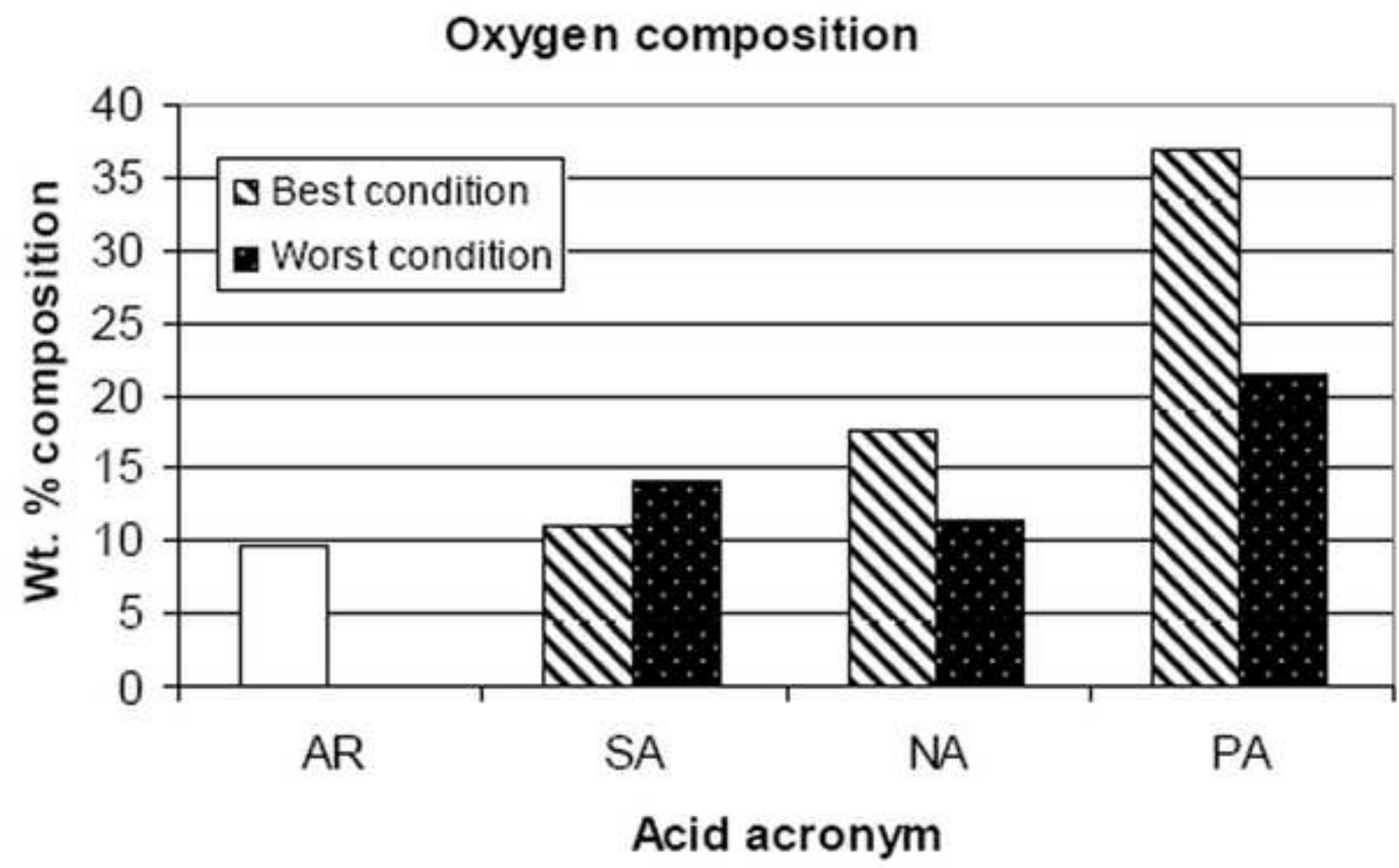


Fig. 10a

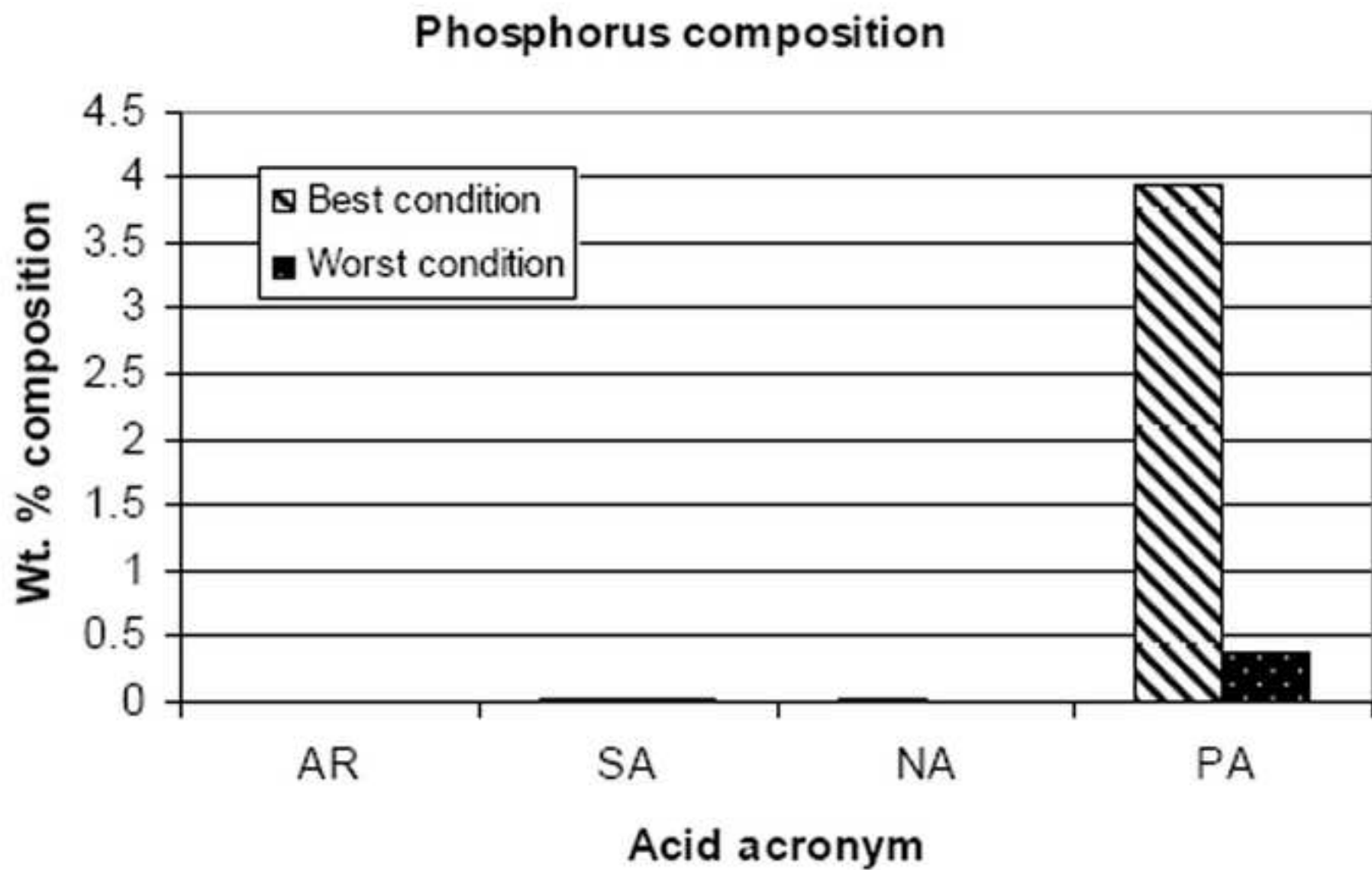


Fig. 10b

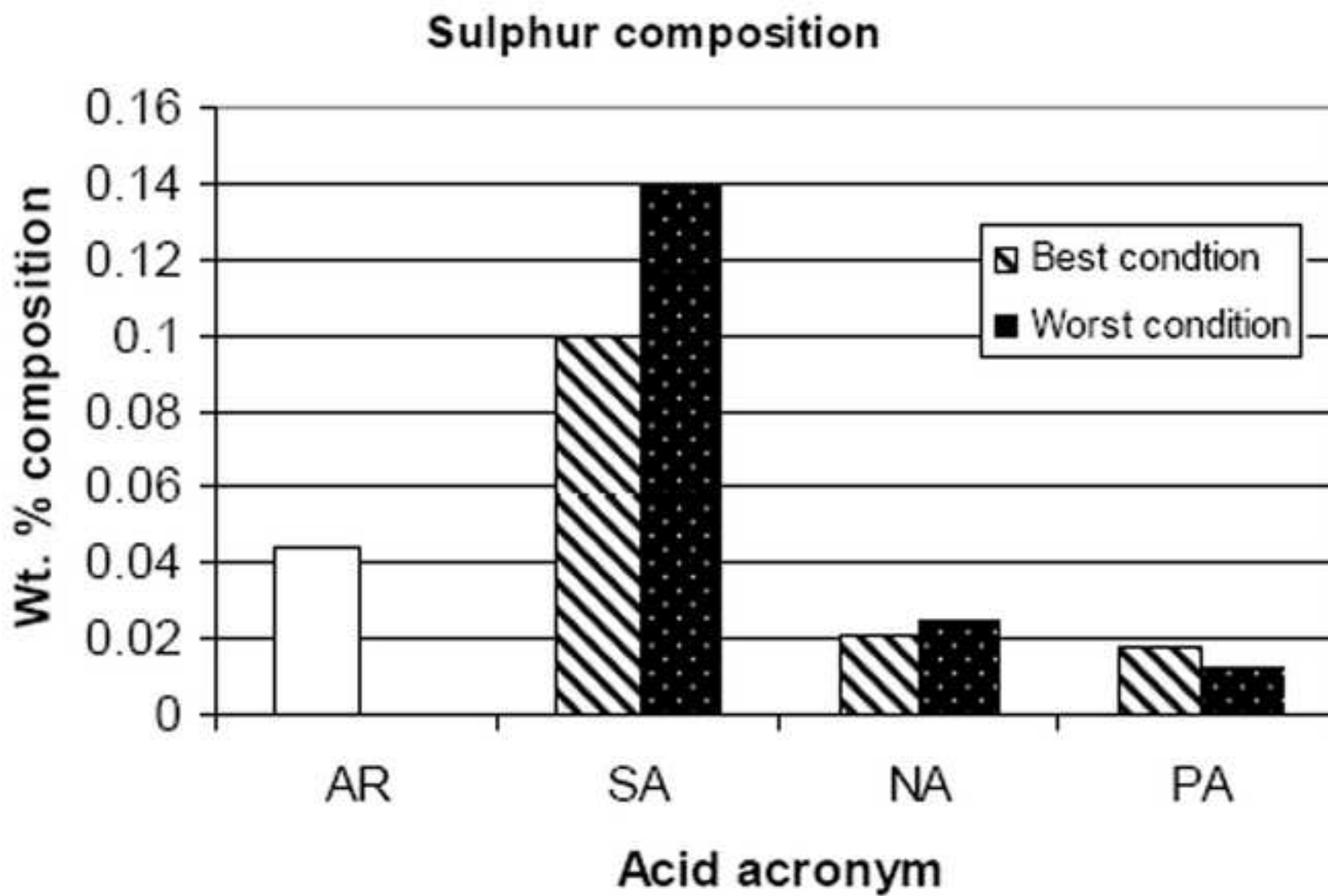


Fig. 10c

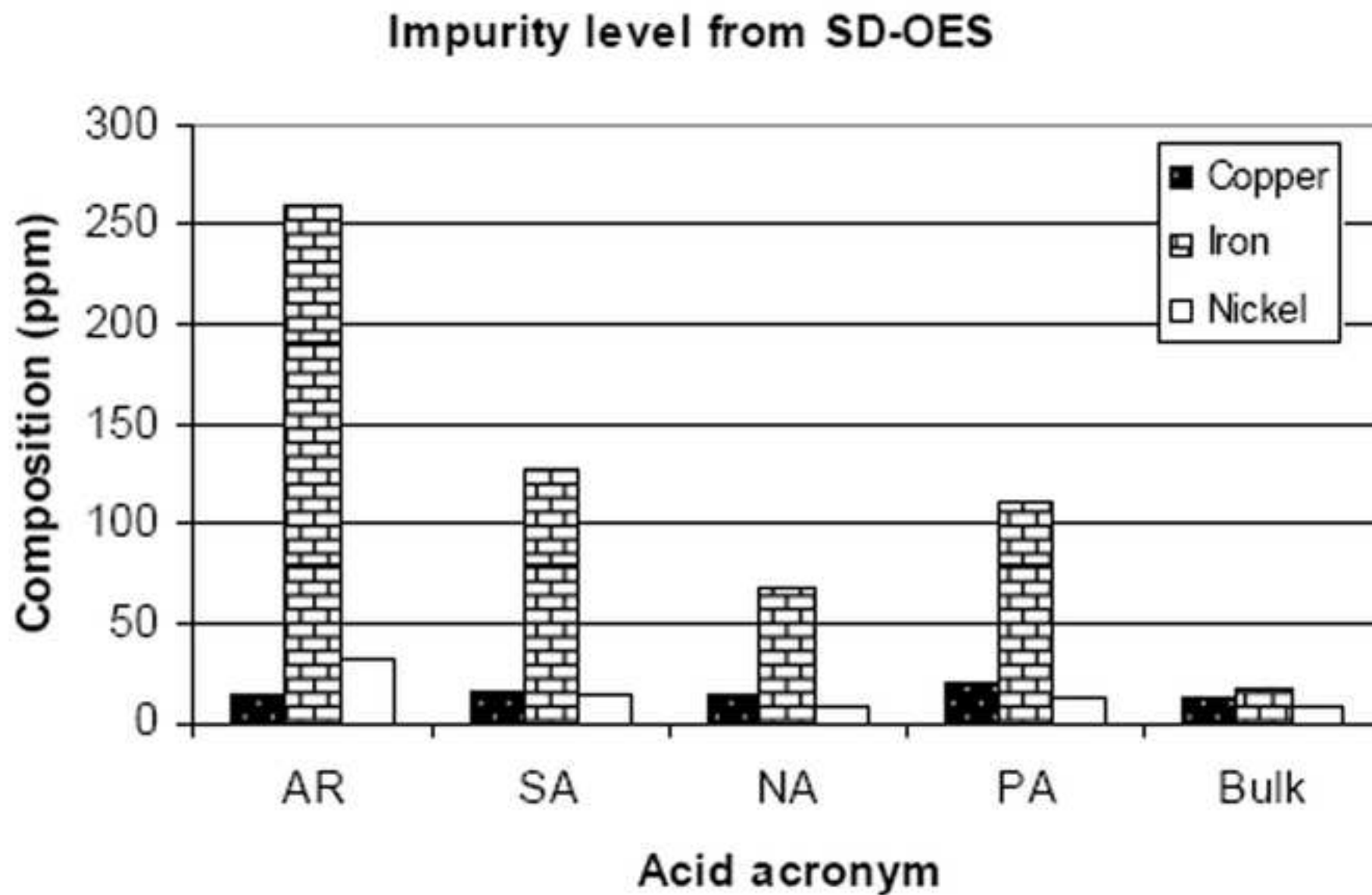


Fig. 11a

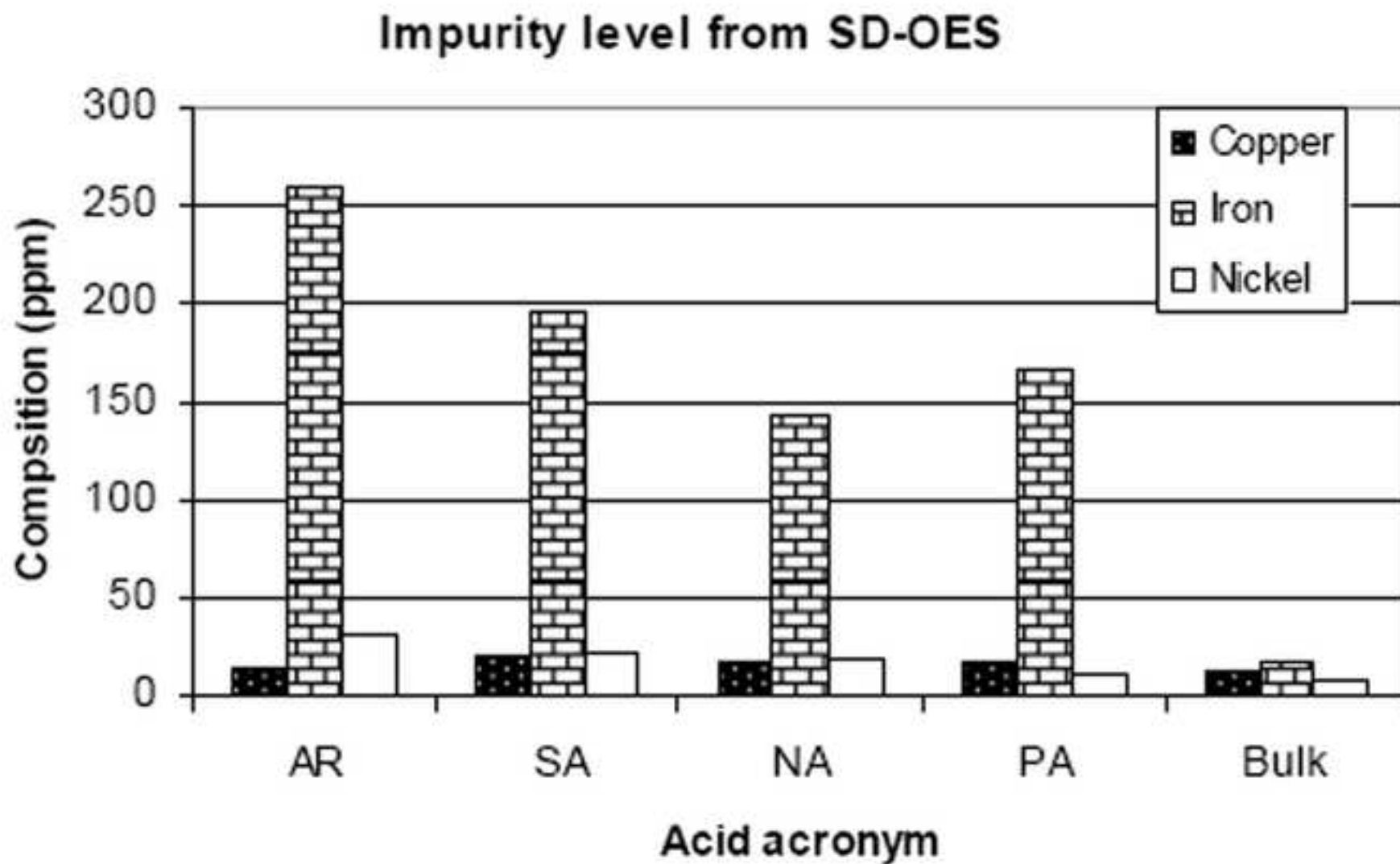


Fig. 11b

Figure 12a

[Click here to download high resolution image](#)

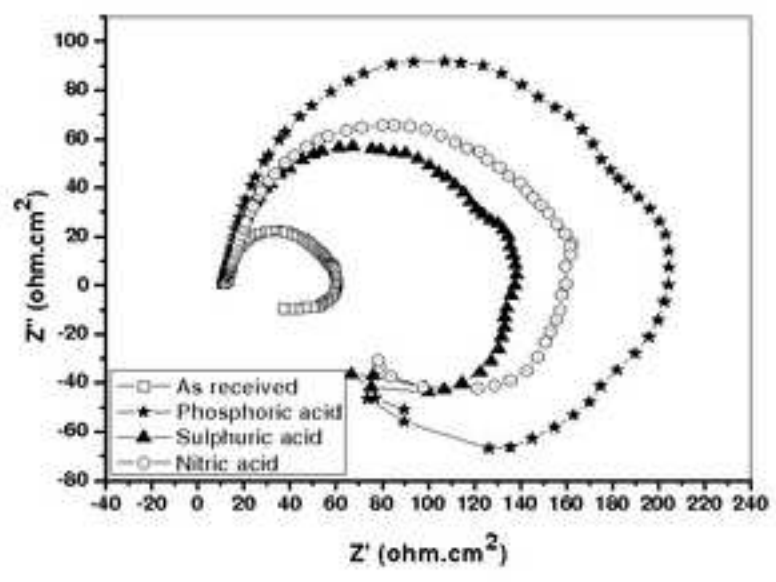


Fig. 12a

Figure 12b

[Click here to download high resolution image](#)

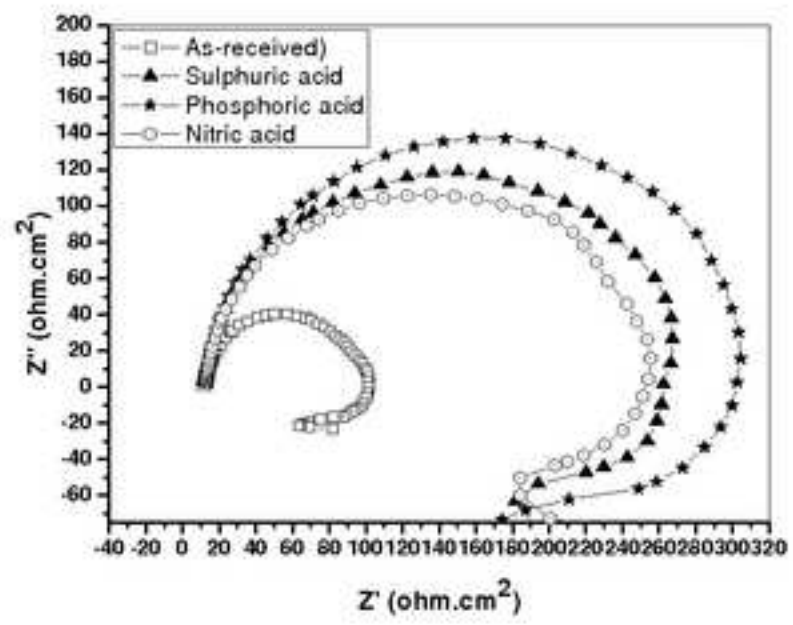


Fig. 12b

Figure 13

[Click here to download high resolution image](#)

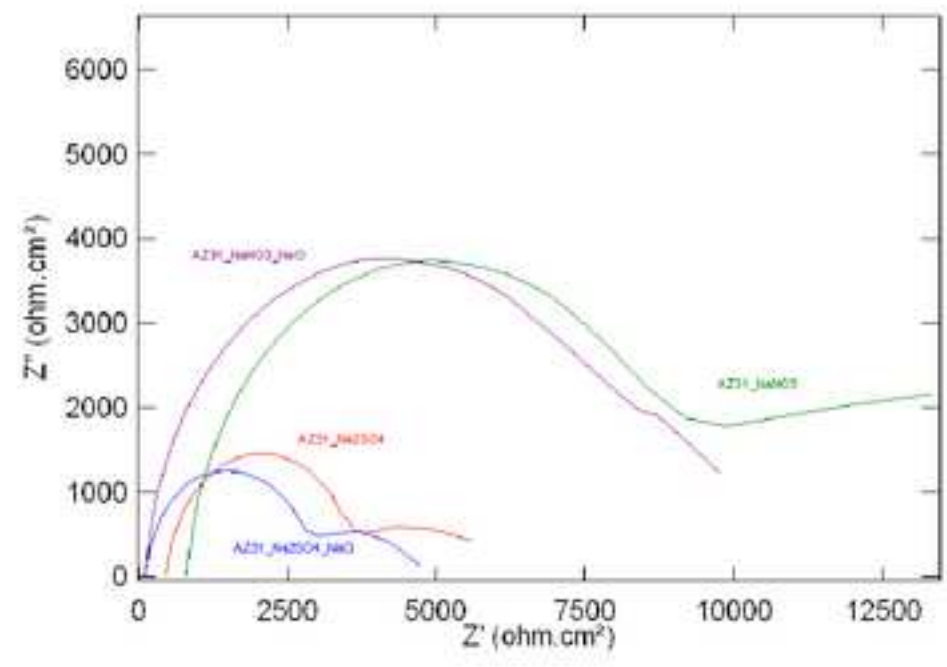


Fig. 13

Table 1: Chemical composition (in wt %) of AZ31 magnesium alloy.

Description		Al	Zn	Mn	Si	Ca	Cu	Ni	Fe	Mg
As-received	Surface	2.97	0.85	0.24	0.02	0.003	0.002	0.004	0.026	Bal.
	Bulk	2.87	0.81	0.25	0.02	0.005	0.001	0.001	0.002	Bal.
	Standard	3.00	1.00	<0.50	<0.10	-	<0.005	<0.002	<0.005	Bal.

Table 2: Bath composition and operating conditions of cleaning AZ 31 Mg alloy sheet.

Process	Operation	Composition of cleaning bath	Conc. (g/l)	pH	Time (s) of immersion in each bath concentration
1	Alkaline cleaning	Sodium hydroxide, NaOH	40	13.6	15, 30, 60, 120
2	Acid cleaning (pickling)	Sulphuric acid, H ₂ SO ₄	10	1.68	
			30	1.38	
			50	1.22	
		Nitric acid, HNO ₃	20	1.39	
			50	1.24	
			80	1.04	
		Phosphoric acid, H ₃ PO ₄	40	1.84	
			60	1.78	
80	1.72				

Table 3: Alloying and impurity elements' phases formed during immersion and solubility conditions in aqueous solutions [17].

	All acid	Ksp	SA	Ksp	NA	Ksp	PA	Ksp
Mg	Mg(OH) ₂	5.61x10 ⁻¹²	MgSO ₄	soluble	Mg(NO ₃) ₂	soluble	Mg ₃ (PO ₄) ₂	1.04x10 ⁻²⁴
Al	Al(OH) ₃	3.0x10 ⁻³	Al ₂ (SO ₄) ₃	soluble	Al(NO ₃) ₃	soluble	AlPO ₄	9.84x10 ⁻²¹
Zn	Zn(OH) ₂	3.0x10 ⁻¹⁷	ZnSO ₄	soluble	Zn(NO ₃) ₂	soluble	Zn ₃ (PO ₄) ₂	slightly soluble
Fe	Fe(OH) ₂	2.64x10 ⁻³⁹	Fe ₂ (SO ₄) ₃	soluble	Fe(NO ₃) ₃	soluble	FePO ₄	9.9 x 10 ⁻¹⁶
Cu	Cu(OH) ₂	insoluble	CuSO ₄	soluble	Cu(NO ₃) ₂	soluble	Cu ₃ (PO ₄) ₂	1.40 x 10 ⁻³⁷
Ni	Ni(OH) ₂	5.47x10 ⁻¹⁶	NiSO ₄	soluble	Ni(NO ₃) ₂	soluble	Ni ₃ (PO ₄) ₂	4.74 x 10 ⁻³²

Table 4: Best conditions for each acid

Acid	Conc. (g/l)	Immersion time (s)	Mat. removed (μm)	Corr. rate (mm/yr)
Sulphuric acid	50	15	6.85 ± 0.85	2.20 ± 0.18
Nitric acid	80	120	8.21 ± 0.11	0.51 ± 0.10
Phosphoric acid	80	60	4.14 ± 0.35	0.74 ± 0.31

Table 5: Worst conditions for each acid

Acid	Conc. (g/l)	Immersion time (s)	Mat. removed (μm)	Corr. rate (mm/yr)
Sulphuric acid	10	120	1.75 ± 0.10	17.16 ± 0.74
Nitric acid	20	15	0.35 ± 0.06	10.10 ± 4.44
Phosphoric acid	40	15	0.76 ± 0.11	7.76 ± 1.00

Table 6: % elemental composition of the points analyzed with EDX for as-received (AR), sulphuric (SA), nitric (NA) and phosphoric (PA) acid treated specimens with the best corrosion behaviour in SST.

Points		Weight % composition															
		C	O	Na	Cu	Mg	Al	Zn	Mn	Si	P	S	Cl	K	Ca	Cr	Fe
AR	P1	-	0.86	-	1.69	93.30	3.33	0.83	-	-	-	-	-	-	-	-	-
	P2	60.79	11.70	-	-	18.11	1.50	-	-	0.30	0.09	0.79	2.35	0.76	0.87	0.43	2.30
	P3	-	7.66	-	-	5.03	0.08	-	-	0.43	-	-	-	-	-	1.07	85.74
	Matrix	-	6.81	-	1.49	87.37	2.52	0.70	-	0.31	-	-	-	-	-	-	0.80
SA	P1	-	31.27	-	1.84	36.29	6.69	-	-	0.41	-	0.80	-	-	-	-	22.70
	P2	-	23.93	2.17	-	41.90	4.61	-	-	0.46	-	0.95	-	-	-	0.28	25.70
	P3	-	8.83	-	-	81.51	3.54	1.32	-	0.79	-	-	-	-	-	0.35	3.66
	Matrix	-	1.81	-	-	93.55	3.41	1.06	0.14	0.08	-	-	-	-	-	-	-
NA	P1	-	24.71	4.17	-	53.80	11.88	4.53	-	0.59	-	-	-	-	-	0.02	0.36
	P2	-	41.16	7.08	-	0.62	11.61	0.13	-	36.74	-	-	-	-	-	0.40	2.27
	P3	3.99	20.02	-	-	5.68	1.14	0.89	-	0.86	-	-	0.36	0.23	11.57	-	55.26
	Matrix	-	4.38	-	-	89.86	4.07	1.49	-	0.19	-	-	-	-	-	-	-
PA	P1	-	3.70	-	-	92.03	3.03	1.09	-	0.15	-	-	-	-	-	-	-
	P2	-	46.79	-	-	47.55	2.50	0.56	0.29	0.77	0.32	-	-	-	-	-	1.21
	P3	-	20.96	-	-	9.07	1.61	0.55	0.98	1.22	0.13	0.15	-	-	-	0.85	64.48
	Matrix	-	35.22	-	-	49.66	7.87	1.87	0.54	0.67	2.92	0.68	-	-	-	-	0.57

REVIEWERS' COMMENTS AND CORRESPONDING CORRECTIONS

REVIEWER #2:

p. 5, 3rd line from the bottom: Is that really 100 μm or should it be 100 nm? If it is really 100 μm , it should be explained why this method can be used to investigate surface impurities.

I removed the word "average" in page 5, in the 7th line from the bottom. Then, I included the text below.

"This implies that the measured elemental composition is only an average over this depth and the real surface contamination is even higher (about 20 x assuming 5 μm depth of severely contaminated surface). Due to the heavy deformation during rolling the contamination is not only restricted to the top surface, thus especially enrichment of heavy metal impurities can be seen, even if they are "diluted" by the larger analyzed volume".

Fig. 11: there seems to be no difference between 11a and 11b!?

As-received (AR) and bulk in both figures are the same as they were not subjected to any pickling treatment.

We expect the differences to show for SA, NA and PA which is conspicuous for iron composition being much higher in Fig 11b than in Fig. 11a. The Ni compositions in Fig. 11a and 11b are 14.3 and 23 respectively for SA and 9.2 and 18.5 respectively for NA. However, for PA Cu composition is higher in Fig. 11a than in Fig. 11b, being 19.1 in Fig.11a and 16 in Fig. 11b while Ni composition is equal in both figures as 11.9. The reason for this is the results for PA shown in Fig. 11a spent more time (60 s) in phosphoric acid than the results shown in Fig 11b (15 s). This longer time gave more allowance for the formation of phosphate coating thereby inhibiting further material removal, making the composition in Fig 11a for PA slightly higher than in Fig. 11b

In summary, there is a difference between Fig. 11a and Fig. 11b. The difference has been made clearer with the change fro 3-D to 2-D style of the charts.

Editor's additional comments:

1. Three-dimensional diagrams should not be used, unless necessary. None of these are necessary. The data of each graph on 3-d graphs should be presented on one 2-d graphs. (Fig. 1)

Fig. 1 (a, b and c) has been changed to 2-D style

2. The bar graphs presented in 3-d style should be presented in 2- style. (Figs 10, 11)

Figs. 10 (a, b and c) and 11 (a and b) have been changed to 2-D style

3. Write equations with proper symbols for parameters, which are defined with units. (Equations 1, 2)

$$W = \frac{w \cdot 10^4}{\rho \cdot A} \quad (1)$$

where W = material removed in μm

w = weightloss in g
 ρ = density in g/cm^3
 A = area in cm^2

$$R = \frac{8.7757 \cdot 10^4 w}{\rho \cdot A \cdot t} \quad (2)$$

where R = corrosion rate in mm/ year
 t = time in hours

Equations 1 and 2 have been written with proper symbols for parameters which are defined with units.

4. Write references in Corrosion Science style.

The references have been written in Corrosion Science style

5. Conclusion should be shortened.

The conclusion has been shortened accordingly.